Sequence Design for Spectral Shaping via Minimization of Regularized Spectral Level Ratio

Linlong Wu and Daniel P. Palomar, *Fellow, IEEE*

***Abstract*—The topic of sequence design has received considerable attention due to its wide applications in active sensing. One important desired property for the design sequence is the spectral shape. In this paper, the sequence design problem is formulated by minimizing the regularized spectral level ratio subject to a peak-to-average power ratio constraint. Then, two algorithms are proposed by combining both the Dinkelbach's algorithm and the majorization–minimzation (MM) method organically. Specifically, by using the Dinkelbach's algorithm, the challenging fractional programming problem can be handled by solving a series of subproblems, which are further solved via the MM method. The numerical experiments verify the effectiveness of the optimization metric and demonstrate the performance of the proposed algorithms compared with the benchmark.**

***Index Terms*—Spectral shaping, sequence design, spectral level ratio, Dinkelbach's algorithm, majorization-minimization, PAR constraint.**

I. Introduction

TRANSMIT sequence plays an important role in many active-sensing applications including communications, sonar, radar, and medical imaging [1]–[3]. For instance, in radar systems, well-designed sequences can allow for a more accurate estimation and a reduced computational cost at the receive side. One important task of sequence design is to adapt the spectrum of the sequence to a changing or pre-specified environment. Specifically, the transmit sequence should avoid certain frequency bands or try to minimize the spectral power on those bands. The motivation behind can be well understood when considering spectrum sharing among radar and telecommunication systems [4]. Due to the ever growing demand of both wireless communication services and accurate remote sensing capabilities, the amount of desired bandwidth is increasing. Consequently, spectral sharing among radar and telecommunications becomes a solution to this significant issue [5], [6]. Signals from other radiation systems on some frequency range of the band can be treated as an interference for radar. In order to avoid the interference or reduce its effect on radar system, it is desired or required that the designed radar waveform has deep notches on those frequency bands. Besides, combining several clear bands together can increase the total system bandwidth so as to improve the range resolution [7]. In addition, from the perspective of the radar signal design, several performance metrics [8]–[10] including spectral property may be also considered jointly to meet the waveform requirements. Therefore, spectral shaping has become a hot research topic in sequence design recently and a lot of works have contributed to it as seen in the burgeoning literature.

From the perspective of problem formulation, the existing works dealing with spectral shaping can be roughly categorized into two categories. In the first category, the spectral requirements are usually formulated as quadratic constraints or quadratic terms of the objective function. As formulated in [11, equation (2)], the quadratic expression represents the spectral energy in certain "forbidden" or stop frequencies. In [12], the total weighted interfering energy transmitted on the stopbands expressed as the weighted sum of quadratic terms was set to be no more than the pre-determined amount of allowed interference. Then the signal-to-interference-plus-noise ratio (SINR) maximization problem including this spectral sharing constraint was solved via semidefinite relaxation (SDR). Then [13] further improved the proposed algorithm by considering a suitable modulation of the transmitted waveform energy. Reference [14] solved the same problem formulated in [12] via the alternating direction method of multipliers (ADMM) with better computational efficiency. Reference [15] extended [12] by jointly considering both the transmit and receive sides. Different from the control on the overall interference energy, [16] enforced a specific control on the interference energy radiated on each shared band. In [17], the weighted stopband power was formulated as a quadratic term of the objective function, then an iterative algorithm based on pattern search was proposed to simultaneously minimize the weighted integrated sidelobe level (ISL) and stopband power. Similarly, [18] aimed at maximizing the SINR and minimizing the stopband power jointly.

In the second category of spectral shaping, the spectral requirements are usually formulated as (part of) the objective function in the least-square form. Specifically, the spectrum of the designed sequence should be forced to be close to a spectral mask in the sense of the least-square error. The spectral mask in fact is the desired spectrum for the designed sequence. A classical formulation was proposed in [19], where a least-square fitting problem was proposed and then extended by allowing the magnitude of the spectral mask within a range. Compared with [19], [20] considered the weighted least squares form and

Manuscript received August 19, 2018; revised January 29, 2019, May 16, 2019, and June 23, 2019; accepted July 2, 2019. Date of publication July 23, 2019; date of current version August 9, 2019. The associate editor coordinating the review of this manuscript and approving it for publication was Prof. Nicolas Gillis. This work was supported by the Hong Kong RGC Theme-based Research Scheme under Grant T21-602/15R. *(Corresponding author: Linlong Wu.)*

The authors are with the Department of Electronic and Computer Engineering, The Hong Kong University of Science and Technology, Hong Kong (e-mail: lwuag@connect.ust.hk; palomar@ust.hk).

Digital Object Identifier 10.1109/TSP.2019.2929468

used the Lagrange programming neural network (LPNN) to solve the general problem. Different from [19], both frequency stopbands and correlation sidelobes were considered in [21], and an efficient algorithm named SCAN was proposed. In [22], both power spectral density (PSD) and autocorrelation function (ACF) masks were set and then jointly optimized. Note that all problems optimizing ACF or ISL [23]–[25] are in fact special cases of this approach since an ideal ACF in time domain corresponds to a flat spectrum in frequency domain. Thus, optimizing the ACF is in fact shaping the corresponding spectrum to be flat. Correspondingly, the spectral mask is set to be the a horizontal line in the whole band [26].

Recently, [27] has proposed an interesting metric for spectral shaping referred as spectral level ratio (SLR), which is the ratio of the maximum stopband level to the minimum passband level. Recall that in the first category of spectral shaping introduced above, before designing the sequence, the thresholds, i.e., the amounts of allowed interference on each sharing bands need to be set. An inappropriate setting of the threshold will raise the issue of feasibility [12]. Similarly, in the second category, the spectral mask or its range of each frequency grid point should also be set in advance, which also need to be chosen carefully. Otherwise, the existence of solution is not guaranteed for a specific spectral shape, and the mask points near sharp spectral jumps need to be carefully reselected or an offset should be used [19]. In addition, in some situations, i.e., the initial stage of the construction of radio environment map (REM) [28], we only know the stopbands and passbands without any further information. Consequently, these masks and thresholds are not easy to set appropriately in advance. Compared with the existing approaches, the SLR proposed in [27] cleverly circumvents those settings of threshold or spectral mask. Thus, this metric and its corresponding algorithms are worth exploring to expand the arsenal for spectral shaping.

In this paper, we adopt this interesting and also quite challenging optimization metric proposed in [27], and modify it to be regularized SLR (RSLR), a more suitable optimization metric for spectrum shaping. Then, a general problem is formulated with consideration of the peak-to-average power ratio (PAR) constraint. For the formulated problem, we propose two iterative algorithms both based on the Dinkelbach's algorithm [29] and the majorization-minimizaiton (MM) method [30], [31]. However, the difference between the two proposed algorithms lies in the approach from the outer Dinkelbach's algorithm to the inner MM method. In addition, the convergence and complexity of each proposed algorithm is analyzed. Experiments show that our method is more efficient than the benchmark and can design a sequence with a desired spectrum shape.

The rest of this paper is organized as follows. In Section II, we formulate the spectrally constrained sequence design problem of interest. In Section III, some preliminaries of the Dinkelbach's algorithm and the MM method are briefly introduced. Two algorithms are then derived in Section IV and Sections V, respectively. At the end of each section, we give a complete description of the derived algorithm and analyze its computational cost and convergence. In Section VII, we analyze the numerical performance of the proposed algorithms and compare them with the existing benchmark. Finally, the conclusions are given in Section VIII.

Notation: $\mathbb{R}^n$ and $\mathbb{C}^n$ denote the n-dimensional real and complex vector space, respectively. $\mathbb{R}^{m\times n}$ and $\mathbb{C}^{m\times n}$ denote the $m \times n$ real and complex matrix space, respectively. $\mathbb{R}_0^+$ and $\mathbb{R}^-$ denote the set of non-negative real numbers and the set of negative real numbers, respectively. Boldface uppercase letters stand for matrices. Boldface lowercase letters stand for column vectors. Standard lowercase letters stand for scalars. $(\mathbf{x})^T$ and $(\mathbf{x})^*$ denote the transpose and conjugate of a complex vector $\mathbf{x}$, respectively. $\mathrm{Re}(\mathbf{x})$ and $\arg(\mathbf{x})$ denote the element-wise real part and the phase of a complex vector $\mathbf{x}$, respectively. $(\mathbf{x})^T$, $(\mathbf{x})^*$, $(\mathbf{x})^H$, $\mathrm{tr}(\mathbf{x})$, $\mathrm{vec}(\mathbf{x})$, $\lambda_{max}(\mathbf{x})$, and $\lambda_u(\mathbf{x})$ denote the transpose, complex conjugate, conjugate transpose, trace, vectorization, largest eigenvalue, and upper bound of the largest eigenvalue of a matrix $\mathbf{X}$, respectively. $\mathrm{Diag}(\mathbf{x})$ stands for a diagonal matrix with its principal diagonal filled with $\mathbf{x}$. $\mathbf{I}_N$ denotes the $N \times N$ identity matrix. $\mathbf{1}_N$ denotes the $N \times 1$ vector with all elements being 1. x_i denotes the i-th element of $\mathbf{x}$. $|\cdot|$ denotes the modulus of a complex scalar or the cardinality of a set, the element-wise modulus of a complex vector, or the number of elements of a set. $\|\cdot\|$ denotes the ℓ_2 norm of a vector. $\otimes$ denotes the Kronecker product.

II. Regularized SLR and Problem Formulation

We aim to design a transmit radar sequence $\mathbf{x} = [x_1, \ldots, x_N]^T \in \mathbb{C}^N$ with length being N, which should have a desired spectrum and satisfy a specific PAR level. Let $\mathcal{S}$ and $\mathcal{P}$ denote the stopband and passband frequency grid set of interest, respectively, which satisfy $\mathcal{S} \cup \mathcal{P} \subseteq \{0, 1, \ldots, N-1\}$ and $\mathcal{S} \cap \mathcal{P} = \emptyset$. Denote the discrete Fourier transform (DFT) matrix by $\mathbf{F}_{DFT} = [\mathbf{f}_0, \ldots \mathbf{f}_{N-1}] \in \mathbb{C}^{N\times N}$, where $\mathbf{f}_\omega = \frac{1}{\sqrt{N}}[1, e^{j2\pi\omega/N}, \ldots, e^{j2\pi\omega(N-1)/N}]^T \in \mathbb{C}^N$ for $\omega = 0, \ldots, N-1$. The minimal passband level and the maximal stopand level can be expressed by $\min\{|\mathbf{f}_\omega^H\mathbf{x}|^2|\omega \in \mathcal{P}\}$ and $\max\{|\mathbf{f}_\omega^H\mathbf{x}|^2|\omega \in \mathcal{S}\}$, respectively. In [27], the spectral level ratio (SLR) is defined as

$$\mathrm{SLR} = \frac{\max\left\{\left|\mathbf{f}_\omega^H\mathbf{x}\right|^2|\omega \in \mathcal{S}\right\}}{\min\left\{\left|\mathbf{f}_\omega^H\mathbf{x}\right|^2|\omega \in \mathcal{P}\right\}}, \tag{1}$$

and the problem is formulated as

$$\begin{aligned} \underset{\mathbf{x}}{\text{minimize}} \quad & \mathrm{SLR} \\ \text{subject to} \quad & |x_n| = 1 \ \text{ for } \ n = 1, \ldots, N. \end{aligned} \tag{2}$$

Intuitively, SLR should be minimized so that $\max\{|\mathbf{f}_\omega^H\mathbf{x}|^2|\omega \in \mathcal{S}\}$ becomes as small as possible and $\min\{|\mathbf{f}_\omega^H\mathbf{x}|^2|\omega \in \mathcal{P}\}$ becomes as large as possible. From the perspective of optimization, it is obvious that problem (2) is optimally solved once $\max\{|\mathbf{f}_\omega^H\mathbf{x}|^2|\omega \in \mathcal{S}\} = 0$. Correspondingly, the optimal solution to problem (2) is $\mathbf{x}^\star \in \mathcal{N}ull(\mathbf{f}_\omega|\omega \in \mathcal{S})$, i.e., the null space of the subspace spanned by $\{\mathbf{f}_\omega\}_{\omega\in\mathcal{S}}$. This cannot guarantee the denominator to be well processed. An extreme example is that $\mathbf{x} = \mathbf{f}_\omega$ for $\forall\omega \in \mathcal{P}$ is also an optimal solution, for which the denominator $\min\{|\mathbf{f}_\omega^H\mathbf{x}|^2|\omega \in \mathcal{P}\}$ might be very small. Note that

if $\{\mathbf{f}_\omega\}_{\omega\in\mathcal{S}\cup\mathcal{P}}$ are not the columns of the DFT matrix $\mathbf{F}_{DFT}$, then SLR is still a good optimization metric for spectral shaping. Note that the above case of $\max\{|\mathbf{f}_\omega^H\mathbf{x}|^2|\omega\in\mathcal{S}\}=0$ only happens for the N point DFT case. If frequency oversampling (more than N frequency samples) is considered for the passbands and stopbands, then the proposed SLR is suitable for optimization.

In order to make the SLR more suitable for optimization, we propose the regularized spectral level ratio (RSLR) as follows:

$$\text{RSLR}=\frac{\max\left\{\left|\mathbf{f}_\omega^H\mathbf{x}\right|^2|\omega\in\mathcal{S}\right\}+c}{\min\left\{\left|\mathbf{f}_\omega^H\mathbf{x}\right|^2|\omega\in\mathcal{P}\right\}}, \tag{3}$$

where c is a positive constant.[1]

Therefore, the problem of interest is formulated as

$$\begin{aligned}\underset{\mathbf{x}}{\text{minimize}}\quad & \text{RSLR}\\ \text{subject to}\quad & \|\mathbf{x}\|_2^2=N,\\ & |x_n|\le\sqrt{\gamma}\quad\text{for}\quad n=1,\ldots,N,\end{aligned} \tag{4}$$

where γ represents the PAR parameter. For simplicity of notation, problem (4) will be expressed as

$$\underset{\mathbf{x}\in\mathcal{X}}{\text{minimize}}\quad\frac{\max\left\{\mathbf{x}^H\mathbf{F}_i\mathbf{x}|i\in\mathcal{S}\right\}+c}{\min\left\{\mathbf{x}^H\mathbf{F}_i\mathbf{x}|i\in\mathcal{P}\right\}}, \tag{5}$$

where $\mathbf{F}_i=\mathbf{f}_i\mathbf{f}_i^H$ and the constraint set is denoted by $\mathcal{X}\triangleq\{\mathbf{x}|\|\mathbf{x}\|_2^2=N,|x_n|\le\sqrt{\gamma}\ \text{ for }\ n=1,\ldots,N\}$.

Before proceeding with the design of the algorithm for problem (5), we make some comments about this problem formulation:

- Compared with the existing approaches, the highlight of this formulation is that it does not require any spectral settings in advance except $\mathcal{S}$ and $\mathcal{P}$.
- The constraint set is more general than the unit modulus constraint, which is a special case when $\gamma=1$. In addition, when $\gamma=N$, only the first constraint $\|\mathbf{x}\|_2^2=N$ takes effect. By increasing the value of γ, we are in fact extending the feasible set, and the optimal objective value should be nonincreasing.
- Generally speaking, we are facing a challenging optimization problem. First, the objective function is fractional. Second, both $\max\{\mathbf{x}^H\mathbf{F}_i\mathbf{x}|i\in\mathcal{S}\}$ and $\min\{\mathbf{x}^H\mathbf{F}_i\mathbf{x}|i\in\mathcal{P}\}$ are nondifferentiable. Third, both the objective function and the constraint set are highly nonconvex. These main difficulties will be handled well when we derive our proposed algorithms.

III. Preliminaries: The Dinkelbach's Algorithm and the MM Method

In this section, we will briefly introduce two algorithmic frameworks which will be used in our algorithm derivation.

[1]Note that $\text{RSLR}=\frac{\max\{|\mathbf{f}_\omega^H\mathbf{x}|^2|\omega\in\mathcal{S}\}+c}{\min\{|\mathbf{f}_\omega^H\mathbf{x}|^2|\omega\in\mathcal{P}\}}=\frac{\max\{|\mathbf{f}_\omega^H\mathbf{x}|^2|\omega\in\mathcal{S}\}}{\min\{|\mathbf{f}_\omega^H\mathbf{x}|^2|\omega\in\mathcal{P}\}}+\frac{c}{\min\{|\mathbf{f}_\omega^H\mathbf{x}|^2|\omega\in\mathcal{P}\}}$. For $\mathbf{x}\in\mathcal{N}ull(\mathbf{f}_\omega|\omega\in\mathcal{S})$, the first term becomes 0. Thus, no matter what value c is, the optimal solution is the one which maximizes $\min\{|\mathbf{f}_\omega^H\mathbf{x}|^2|\omega\in\mathcal{P}\}$ with $\mathbf{x}\in\mathcal{N}ull(\mathbf{f}_\omega|\omega\in\mathcal{S})$.

A. The Dinkelbach's Algorithm

The Dinkelbach's algorithm, first proposed in [29], is a powerful optimization scheme dealing with nonlinear fractional programming problems, which has already been studied in many applications [32]. The idea behind it is to convert, by introducing an auxiliary variable, the original nonlinear fractional problem into a sequence of non-fractional problems to be solved until convergence.

Consider a general fractional programming problem

$$\begin{aligned}\underset{\mathbf{x}}{\text{minimize}}\quad & \frac{f_1(\mathbf{x})}{f_2(\mathbf{x})}\\ \text{subject to}\quad & \mathbf{x}\in\mathcal{X}.\end{aligned} \tag{6}$$

where $f_2(\mathbf{x})>0$ for $\mathbf{x}\in\mathcal{X}$. Suppose the problem is hard to directly minimize. Following the general idea of the Dinkelbach's algorithm, we need to solve the following problem at the k-th iteration,

$$\begin{aligned}\underset{\mathbf{x}}{\text{minimize}}\quad & f_1(\mathbf{x})-y_kf_2(\mathbf{x})\\ \text{subject to}\quad & \mathbf{x}\in\mathcal{X},\end{aligned} \tag{7}$$

where y_k is the auxiliary variable updated as

$$y_k=\frac{f_1(\mathbf{x}_k)}{f_2(\mathbf{x}_k)}. \tag{8}$$

Assume the optimal solution of problem (7) is $\mathbf{x}_{k+1}$. One advantage of the Dinkelbach's algorithm is the guarantee of monotonicity of the sequence $\{\frac{f_1(\mathbf{x}_{k+1})}{f_2(\mathbf{x}_{k+1})}\}$. Since

$$f_1(\mathbf{x}_{k+1})-y_kf_2(\mathbf{x}_{k+1})\le f_1(\mathbf{x}_k)-y_kf_2(\mathbf{x}_k)=0, \tag{9}$$

we have

$$y_{k+1}=\frac{f_1(\mathbf{x}_{k+1})}{f_2(\mathbf{x}_{k+1})}\le y_k=\frac{f_1(\mathbf{x}_k)}{f_2(\mathbf{x}_k)}. \tag{10}$$

Thus, by alternatively solving problem (7) and updating y_k by (8), the convergence is guaranteed because y_k is nonincreasing. Also note that the monotonicity can still be guaranteed as long as $f_1(\mathbf{x}_{k+1})-y_kf_2(\mathbf{x}_{k+1})\le 0$ is satisfied even if $\mathbf{x}_{k+1}$ is not the optimal solution of problem (7). Specially, if $f_1(\mathbf{x})$ is convex and $f_2(\mathbf{x})$ is concave in the convex set $\mathcal{X}$, the overall iterative algorithm will converge to the global optimum solution of problem (6) [33]. For more details about convergence, interested readers may refer to [34], [35].

B. The MM Method

The MM method is a powerful optimization scheme, especially when the problem is hard to tackle directly. The idea behind the MM algorithm is to convert the original problem into a sequence of simpler problems to be solved until convergence.

Consider a general optimization problem

$$\begin{aligned}\underset{\mathbf{x}}{\text{minimize}}\quad & f(\mathbf{x})\\ \text{subject to}\quad & \mathbf{x}\in\mathcal{X}.\end{aligned} \tag{11}$$

Suppose the problem is hard to directly minimize. Following the general MM idea at the ℓ-th iteration, we first construct $u(\mathbf{x},\mathbf{x}_\ell)$,

the so-called majorizer of $f(\mathbf{x})$, satisfying the following two requirements at the point $\mathbf{x}_\ell$:

$$u\left(\mathbf{x}, \mathbf{x}_\ell\right) \geq f(\mathbf{x}), \quad \text{for all} \quad \mathbf{x} \in \mathcal{X} \tag{12}$$

$$u\left(\mathbf{x}_\ell, \mathbf{x}_\ell\right) = f\left(\mathbf{x}_\ell\right). \tag{13}$$

Then the MM update is given by

$$\mathbf{x}_{\ell+1} = \underset{\mathbf{x}\in\mathcal{X}}{\operatorname{argmin}}\, u\left(\mathbf{x}, \mathbf{x}_\ell\right). \tag{14}$$

One interesting and useful property of MM based methods is monotonicity:

$$f\left(\mathbf{x}_{\ell+1}\right) \leq u\left(\mathbf{x}_{\ell+1}, \mathbf{x}_\ell\right) \leq u\left(\mathbf{x}_\ell, \mathbf{x}_\ell\right) = f\left(\mathbf{x}_\ell\right), \tag{15}$$

where the first inequality follows from (12), the second one follows from (14) and the last equality follows from (13). Note that from (15), we see that even if $\mathbf{x}_{\ell+1}$ is not the minimizer of $u(\mathbf{x}, \mathbf{x}_\ell)$, the monotonicity can still be guaranteed as long as it improves the function $u(\mathbf{x}_{\ell+1}, \mathbf{x}_\ell) \leq u(\mathbf{x}_\ell, \mathbf{x}_\ell)$, where the equality means the algorithm has already found a stationary point $\mathbf{x}_{\ell+1}$. Thus, the convergence is guaranteed because $f(\mathbf{x}_\ell)$ is nonincreasing after each iteration. For more details about the convergence of $\{f(\mathbf{x}_\ell)\}$ and $\{\mathbf{x}_\ell\}$, interested readers may refer to [31], [36].

The counterpart for maximization problems is referred to as minorization-maximization, of which the key step is to construct a so-called minorizer. The analysis is straightforward by referring to that of the majorization-minimizaiton case above and thus omitted here.

IV. Approximate Iterative Method for Spectrum Shaping

In this section, based on the introduced algorithmic frameworks, an iterative method is proposed to solve problem (5). At the end of this section, we will summarize the derived method and analyze its complexity and convergence.

A. Approximation of the Point-Wise Maximum

At the k-th iteration of the Dinkelbach's algorithm, we have the following problem:

$$\underset{\mathbf{x}\in\mathcal{X}}{\text{minimize}} \quad \max\left\{\mathbf{x}^H\mathbf{F}_i\mathbf{x} | i \in \mathcal{S}\right\} - y_k \min\left\{\mathbf{x}^H\mathbf{F}_i\mathbf{x} | i \in \mathcal{P}\right\}. \tag{16}$$

Due to $y_k = \frac{\max\{\mathbf{x}_k^H\mathbf{F}_i\mathbf{x}_k | i\in\mathcal{S}\}+c}{\min\{\mathbf{x}_k^H\mathbf{F}_i\mathbf{x}_k | i\in\mathcal{P}\}} \geq 0$, problem (16) is equivalent to

$$\underset{\mathbf{x}\in\mathcal{X}}{\text{minimize}} \quad \max\left\{\mathbf{x}^H\mathbf{F}_i\mathbf{x} | i \in \mathcal{S}\right\} + y_k \max\left\{-\mathbf{x}^H\mathbf{F}_i\mathbf{x} | i \in \mathcal{P}\right\}. \tag{17}$$

The objective function is nonconvex and nondifferentiable.

Lemma 1: Denote the objective function of problem (17) by $f(\mathbf{x})$. Then $f(\mathbf{x})$ can be approximated by

$$g(\mathbf{x}) \approx \alpha \log \sum_{i\in\mathcal{S}} \exp\left(\frac{\mathbf{x}^H\mathbf{F}_i\mathbf{x}}{\alpha}\right) + \alpha y_k \log \sum_{i\in\mathcal{P}} \exp\left(-\frac{\mathbf{x}^H\mathbf{F}_i\mathbf{x}}{\alpha}\right) \tag{18}$$

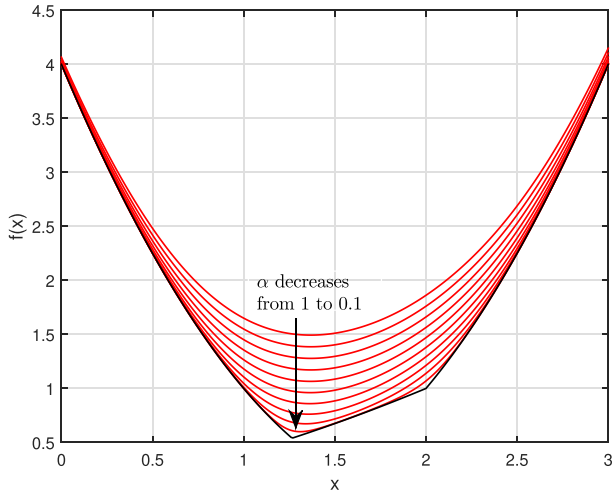

Fig. 1. Approximation of the point-wise maximum with respect to different α. Black: $f(x) = \max\{f_i(x) | i = 1, 2, 3\}$; Red: $g(x) = \alpha \log \sum_{i=1}^{3} \exp\left(\frac{f_i(x)}{\alpha}\right)$, where $f_1(x) = x^2 - 2x + 1$, $f_2(x) = x^2 - 4x + 4$ and $f_3(x) = 0.1x^2 + 0.3x$.

with $f(\mathbf{x}) \leq g(\mathbf{x}) \leq f(\mathbf{x}) + \alpha(\log|\mathcal{S}| + y_k \log|\mathcal{P}|)$, where $\alpha > 0$ is a constant.

Proof: See Appendix A ■

Note that Lemma 1 provides a differentiable approximation of the objective function, and the degree of this approximation can be adjusted by α. Figure 1 shows a toy example for intuitive illustration of this approximation. It is clear that the smaller the value of α, the better the approximation.

By using Lemma 1 and ignoring the constant, the approximate problem is given by

$$\begin{aligned}\underset{\mathbf{x}\in\mathcal{X}}{\text{minimize}} \quad & \log \sum_{i\in\mathcal{S}} \exp\left(\frac{\mathbf{x}^H\mathbf{F}_i\mathbf{x}}{\alpha}\right) \\ & + y_k \log \sum_{i\in\mathcal{P}} \exp\left(-\frac{\mathbf{x}^H\mathbf{F}_i\mathbf{x}}{\alpha}\right),\end{aligned} \tag{19}$$

where the objective function is now differentiable but still nonconvex. In the next two subsections, we will solve problem (19) by applying the MM method.

B. Majorizer Construction

For the first term $\log \sum_{i\in\mathcal{S}} \exp(\frac{\mathbf{x}^H\mathbf{F}_i\mathbf{x}}{\alpha})$ in problem (19), we have

$$\begin{aligned}& \log \sum_{i\in\mathcal{S}} \exp\left(\frac{\mathbf{x}^H\mathbf{F}_i\mathbf{x}}{\alpha}\right) \\ &= \log \sum_{i\in\mathcal{S}} \exp\left(\frac{\mathbf{x}^H\left(\mathbf{F}_i - (1+\epsilon)\mathbf{I}\right)\mathbf{x}}{\alpha} + \frac{(1+\epsilon)\mathbf{x}^H\mathbf{x}}{\alpha}\right) \\ &= \frac{(1+\epsilon)N}{\alpha} + \log \sum_{i\in\mathcal{S}} \exp\left(-\frac{\mathbf{x}^H\left((1+\epsilon)\mathbf{I} - \mathbf{F}_i\right)\mathbf{x}}{\alpha}\right),\end{aligned} \tag{20}$$

where ϵ is a small positive value and we set $\epsilon = 1 \times 10^{-3}$ hereafter. Similarly, for the second term, we have

$$\log \sum_{j\in\mathcal{P}} \exp\left(-\frac{\mathbf{x}^H \mathbf{F}_j \mathbf{x}}{\alpha}\right) = \frac{\epsilon N}{\alpha} + \log \sum_{i\in\mathcal{S}} \exp\left(-\frac{\mathbf{x}^H \left(\mathbf{F}_i + \epsilon \mathbf{I}\right) \mathbf{x}}{\alpha}\right). \quad (21)$$

Thus, by defining $\tilde{\mathbf{F}}_i = \frac{1}{\alpha}((1+\epsilon)\mathbf{I} - \mathbf{F}_i) \succ \mathbf{0}$ and $\hat{\mathbf{F}}_j = \frac{1}{\alpha}(\mathbf{F}_i + \epsilon\mathbf{I}) \succ \mathbf{0}$, problem (19) is equivalent to

$$\begin{aligned} \underset{\mathbf{x}\in\mathcal{X}}{\text{minimize}} \quad & \log \sum_{i\in\mathcal{S}} \exp\left(-\mathbf{x}^H \tilde{\mathbf{F}}_i \mathbf{x}\right) \\ & + y_k \log \sum_{j\in\mathcal{P}} \exp\left(-\mathbf{x}^H \hat{\mathbf{F}}_j \mathbf{x}\right), \end{aligned} \quad (22)$$

Since both terms of the objective function of problem (22) have the same structure, we focus on constructing the majorizer of $\log \sum_{i\in\mathcal{S}} \exp(-\mathbf{x}^H \tilde{\mathbf{F}}_i \mathbf{x})$ for illustration.

Lemma 2: At the ℓ-th iteration, $\log \sum_{i\in\mathcal{S}} \exp(-\mathbf{x}^H \tilde{\mathbf{F}}_i \mathbf{x})$ can be majorized by

$$\log \sum_{i\in\mathcal{S}} \exp\left(-\mathbf{x}^H \tilde{\mathbf{F}}_i \mathbf{x}\right) \le 2\mathrm{Re}\left[\left(\sum_{i\in\mathcal{S}} \mathbf{A}_i^\ell \mathbf{x}_\ell\right)^H \mathbf{x}\right] + \text{constant} \quad (23)$$

with

$$\mathbf{A}_i^\ell = -\frac{\exp\left(-\mathbf{x}_\ell^H \tilde{\mathbf{F}}_i \mathbf{x}_\ell\right) \tilde{\mathbf{F}}_i + \frac{1}{\alpha^2}\left((1+\epsilon)^2 N - 2\epsilon - 1\right) \mathbf{x}_\ell \mathbf{x}_\ell^H}{\sum_{i\in\mathcal{S}} \exp\left(-\mathbf{x}_\ell^H \tilde{\mathbf{F}}_i \mathbf{x}_\ell\right)}. \quad (24)$$

The equality is achieved when $\mathbf{x} = \mathbf{x}_\ell$.

Proof: See Appendix B. ■

Same techniques can be applied on the second term of the objective function of problem (22). we have

$$\log \sum_{i\in\mathcal{P}} \exp\left(-\mathbf{x}^H \hat{\mathbf{F}}_i \mathbf{x}\right) \le 2\mathrm{Re}\left[\left(\sum_{i\in\mathcal{P}} \mathbf{B}_i^\ell \mathbf{x}_\ell\right)^H \mathbf{x}\right] + \text{constant}, \quad (25)$$

where the equality is achieved when $\mathbf{x} = \mathbf{x}_\ell$, and

$$\mathbf{B}_i^\ell = -\frac{\exp\left(-\mathbf{x}_\ell^H \hat{\mathbf{F}}_i \mathbf{x}_\ell\right) \hat{\mathbf{F}}_j + \frac{1}{\alpha^2}\left(\epsilon^2 N + 2\epsilon + 1\right) \mathbf{x}_\ell \mathbf{x}_\ell^H}{\sum_{i\in\mathcal{P}} \exp\left(-\mathbf{x}_\ell^H \hat{\mathbf{F}}_i \mathbf{x}_\ell\right)}. \quad (26)$$

Therefore, the final majorized problem of problem (22) is

$$\begin{aligned} \underset{\mathbf{x}}{\text{minimize}} \quad & \mathrm{Re}\left(\mathbf{p}_\ell^H \mathbf{x}\right) \\ \text{subject to} \quad & \|\mathbf{x}\|_2^2 = N. \\ & |x_n| \le \sqrt{\gamma} \ \text{ for } \ n = 1, \ldots, N, \end{aligned} \quad (27)$$

where

$$\mathbf{p}_\ell = \left(\sum_{i\in\mathcal{S}} \mathbf{A}_i^\ell + y_k \sum_{i\in\mathcal{P}} \mathbf{B}_i^\ell\right) \mathbf{x}_\ell. \quad (28)$$

C. Optimal Solution of the Majorized Problem

For problem (27) with a linear objective function, an closed-form solution has been constructed in [37], which is rewritten and presented as follows:

$$\mathbf{x}^\star = \mathcal{A}_\mathcal{X}\left(\mathbf{p}_\ell\right) \quad (29)$$

where

$$\begin{aligned} \mathcal{A}_\mathcal{X}(\cdot) = & -\left(\mathbf{1}_{\mathbb{R}_0^+}\left(N - m\gamma\right)\right)\sqrt{\gamma}\mathbf{u}_m \odot e^{j\arg(\cdot)} \\ & -\left(\mathbf{1}_{\mathbb{R}^-}\left(N - m\gamma\right)\right)\min\{\beta|\mathbf{z}|, \sqrt{\gamma}\mathbf{1}\} \odot e^{j\arg(\cdot)}, \end{aligned} \quad (30)$$

$\min\{\cdot,\cdot\}$, $|\cdot|$ and $e^{j\arg(\cdot)}$ are element-wise operations, m is the number of nonzero elements of $\mathbf{p}_\ell$,

$$\mathbf{1}_A(x) = \begin{cases} 1, & \text{if } x \in A, \\ 0, & \text{otherwise}, \end{cases} \quad (31)$$

$$\mathbf{u}_m = \Bigg[\underbrace{1, \ldots 1}_{m}, \underbrace{\sqrt{\frac{N - m\gamma}{N\gamma - m\gamma}}, \ldots, \sqrt{\frac{N - m\gamma}{N\gamma - m\gamma}}}_{N-m}\Bigg]^T, \quad (32)$$

$$\begin{aligned} \beta \in & \left\{\beta | \sum_{n=1}^{N} \min\left\{\beta^2 |z_n|^2, \gamma\right\}\right. \\ & \left. = N, \beta \in \left[0, \frac{\sqrt{\gamma}}{\min\{|z_n| \,|\, |z_n| \neq 0\}}\right]\right\}. \end{aligned} \quad (33)$$

Note that the scalar β can be calculated by the bisection method in practice, which should be efficient because it is already known that $\beta \in [0, \frac{\sqrt{\gamma}}{\min\{|z_n| \,|\, |z_n| \neq 0\}}]$. In addition, for the special case where $\gamma = 1$, the constraint set is reduced to the unit-modulus constraint. Then the optimal solution is

$$\mathbf{x}^\star = -e^{j\arg(\mathbf{p}_\ell)}. \quad (34)$$

For the other special case where $\gamma = N$, only the constraint $\|\mathbf{x}\|_2^2 = N$ takes effect, and the optimal solution is

$$\mathbf{x}^\star = -\frac{\sqrt{N}\mathbf{p}}{\|\mathbf{p}\|_2}. \quad (35)$$

D. Complexity and Convergence Analysis

The complete description of the proposed algorithm named as **A**pproximate **I**terative Method for **S**pectrum **S**haping (AISS) is shown in Algorithm 1. It is clear that the main computation of each iteration is the calculation of $\mathbf{p}_\ell$, which consists of $\mathbf{A}_i^\ell \mathbf{x}_\ell$ for all $i \in \mathcal{S}$ and $\mathbf{B}_i^\ell \mathbf{x}_\ell$ for all $i \in \mathcal{P}$. Note that both $\mathbf{A}_i^\ell \mathbf{x}_\ell$ and $\mathbf{B}_i^\ell \mathbf{x}_\ell$ include $\mathbf{f}_\omega^H \mathbf{x}_\ell$ for $\omega \in \mathcal{S} \cup \mathcal{P}$, which can be implemented via the fast Fourier transform (FFT). Thus, the computation cost per iteration is $\mathcal{O}(NlogN)$.

As illustrated in the preliminary part, both the Dinkelbach's algorithm and the MM method can guarantee the monotonicity

Algorithm 1: The Approximate Iterative Method for Spectrum Shaping (AISS).

Require: The stopband $\mathcal{S}$ and passband $\mathcal{P}$.

1) Set $k=0$, initialize $\mathbf{x}_0$
2) **Repeat**
3) Set $\ell=0$, $\mathbf{s}_\ell=\mathbf{x}_k$
4) $y_k=\frac{\max\left\{\mathbf{x}_k^H\mathbf{F}_i\mathbf{x}_k|i\in\mathcal{S}\right\}+c}{\min\left\{\mathbf{x}_k^H\mathbf{F}_i\mathbf{x}_k|i\in\mathcal{P}\right\}}$
5) **Repeat**
6) Calculate $\mathbf{f}_\omega^H\mathbf{s}_\ell$ for all $\omega\in\mathcal{S}\cup\mathcal{P}$
7) $\sum_{i\in\mathcal{S}}\mathbf{A}_i^\ell\mathbf{s}_\ell=\left[\frac{\sum_{i\in\mathcal{S}}\exp\left(\frac{1}{\alpha}\left|\mathbf{f}_i^H\mathbf{s}_\ell\right|^2\right)\mathbf{f}_i^H\mathbf{s}_\ell}{\alpha\sum_{i\in\mathcal{S}}\left(\exp\left(\frac{1}{\alpha}\left|\mathbf{f}_i^H\mathbf{s}_\ell\right|^2\right)\right)}\mathbf{f}_i-\left(\frac{1+\epsilon}{\alpha}+\frac{\left((1+\epsilon)^2N-2\epsilon-1\right)N|\mathcal{S}|\exp\left(\frac{1+\epsilon}{\alpha}N\right)}{\alpha^2\sum_{i\in\mathcal{S}}\exp\left(\frac{1}{\alpha}\left|\mathbf{f}_i^H\mathbf{s}_\ell\right|^2\right)}\right)\mathbf{s}_\ell\right]$
8) $\sum_{i\in\mathcal{P}}\mathbf{B}_i^\ell\mathbf{s}_\ell=\left[-\frac{\sum_{i\in\mathcal{P}}\exp\left(-\frac{1}{\alpha}\left|\mathbf{f}_i^H\mathbf{s}_\ell\right|^2\right)\mathbf{f}_i^H\mathbf{s}_\ell}{\alpha\sum_{i\in\mathcal{P}}\left(\exp\left(-\frac{1}{\alpha}\left|\mathbf{f}_i^H\mathbf{s}_\ell\right|^2\right)\right)}\mathbf{f}_i-\left(\frac{\epsilon}{\alpha}+\frac{\left(\epsilon^2N+2\epsilon+1\right)N|\mathcal{P}|\exp\left(\frac{\epsilon}{\alpha}N\right)}{\alpha^2\sum_{i\in\mathcal{P}}\exp\left(-\frac{1}{\alpha}\left|\mathbf{f}_i^H\mathbf{s}_\ell\right|^2\right)}\right)\mathbf{s}_\ell\right]$
9) $\mathbf{p}_\ell=\left(\sum_{i\in\mathcal{S}}\mathbf{A}_i^\ell\mathbf{s}_\ell+y_k\sum_{i\in\mathcal{P}}\mathbf{B}_i^\ell\mathbf{s}_\ell\right)$
10) Obtain $\mathbf{x}_{\ell+1}$ according to (29).
11) $\ell\leftarrow\ell+1$
12) **Until** convergence
13) $\mathbf{x}_{k+1}=\mathbf{s}_\ell$
14) $k\leftarrow k+1$
15) **Until** convergence

of the sequence of the objective value. However, at the k-th iteration of the Dinkelbach's algorithm, we in fact solve an approximate problem instead of the standard one. Thus, the existing result about the monotonicity cannot be applied directly. In the following lemma, we analyze the monotonicity of the proposed AISS.

Lemma 3: For the generated sequence $\{y_k\}$, we have

$$y_{k+1}-y_k\leq\alpha\frac{\log|\mathcal{S}|+y_k\log|\mathcal{P}|}{\min\left\{\mathbf{x}_{k+1}^H\mathbf{F}_i\mathbf{x}_{k+1}|i\in\mathcal{P}\right\}}. \tag{36}$$

Proof: Let $f_1(\mathbf{x})=\max\{\mathbf{x}^H\mathbf{F}_i\mathbf{x}|i\in\mathcal{S}\}$, $f_2(\mathbf{x})=\min\{\mathbf{x}^H\mathbf{F}_i\mathbf{x}|i\in\mathcal{P}\}$, and $h(\mathbf{x})=\log\sum_{i\in\mathcal{S}}\exp(\mathbf{x}^H\mathbf{F}_i\mathbf{x}/\alpha)+y_k\log\sum_{i\in\mathcal{P}}\exp(-\mathbf{x}^H\mathbf{F}_i\mathbf{x}/\alpha)$. According to Lemma 1, we have the following two inequalities

$$f_1(\mathbf{x})\leq\alpha\log\sum_{i\in\mathcal{S}}\exp\left(\mathbf{x}^H\mathbf{F}_i\mathbf{x}/\alpha\right)\leq f_1(\mathbf{x})+\alpha\log|\mathcal{S}|, \tag{37}$$

$$-f_2(\mathbf{x})\leq\alpha\log\sum_{i\in\mathcal{P}}\exp\left(-\mathbf{x}^H\mathbf{F}_i\mathbf{x}/\alpha\right)\leq-f_2(\mathbf{x})+\alpha\log|\mathcal{P}|. \tag{38}$$

Thus,

$$\begin{aligned}f_1(\mathbf{x})-y_kf_2(\mathbf{x})&\leq\alpha h(\mathbf{x})\\&\leq f_1(\mathbf{x})-y_kf_2(\mathbf{x})+\alpha(\log|\mathcal{S}|+y_k\log|\mathcal{P}|).\end{aligned} \tag{39}$$

Recall that at the k-th iteration, the initial point is $\mathbf{x}_k$ and $y_k=\frac{f_1(\mathbf{x}_k)}{f_2(\mathbf{x}_k)}$. Assume that the output of the k-th iteration is $\mathbf{x}_{k+1}$. We have two possible situations for $\mathbf{x}_{k+1}$:

1) $h(\mathbf{x}_{k+1})\leq 0$. Then $f_1(\mathbf{x}_{k+1})-y_kf_2(\mathbf{x}_{k+1})\leq\alpha h(\mathbf{x}_{k+1})\leq 0$. So $\frac{f_1(\mathbf{x}_{k+1})}{f_2(\mathbf{x}_{k+1})}=y_{k+1}\leq y_k$;

2) $h(\mathbf{x}_{k+1})>0$. Then $f_1(\mathbf{x}_{k+1})-y_kf_2(\mathbf{x}_{k+1})\leq\alpha h(\mathbf{x}_{k+1})$, which is equivalent to

$$y_{k+1}=\frac{f_1(\mathbf{x}_{k+1})}{f_2(\mathbf{x}_{k+1})}\leq y_k+\frac{\alpha h(\mathbf{x}_{k+1})}{f_2(\mathbf{x}_{k+1})}. \tag{40}$$

Since $\mathbf{x}_k$ is the input for the k-th iteration and we are using the MM method which guarantees the monotonicity, we have $h(\mathbf{x}_{k+1})\leq h(\mathbf{x}_k)$. Besides, we have $\alpha h(\mathbf{x}_k)\leq f_1(\mathbf{x}_k)-y_kf_2(\mathbf{x}_k)+\alpha(\log|\mathcal{S}|+y_k\log|\mathcal{P}|)$, which is based on Lemma 1. Thus, (40) can be further relaxed to (also using the equation $f_1(\mathbf{x}_k)-y_kf_2(\mathbf{x}_k)=0$)

$$y_{k+1}\leq y_k+\frac{\alpha(\log|\mathcal{S}|+y_k\log|\mathcal{P}|)}{\min\left\{\mathbf{x}_{k+1}^H\mathbf{F}_i\mathbf{x}_{k+1}|i\in\mathcal{P}\right\}}. \tag{41}$$

The proof is complete. ■

Remark 4: Lemma (3) provides a loose upper bound of $y_{k+1}-y_k$, which is related to the parameter α. Specifically, the smaller the value of α, the smaller the upper bound. In the extreme, $y_{k+1}\leq y_k$ is always guaranteed if $\alpha\to 0$. This is very intuitive because when α becomes smaller, the approximate function becomes closer to the original one. Thus the procedure of the standard Dinkelbach's algorithm is strictly conducted and consequently, the monotonicity is guaranteed.

Remark 5: If $h(\mathbf{x}_{k+1})\leq 0$, then $y_{k+1}\leq y_k$. But even when $h(\mathbf{x}_{k+1})>0$, $y_{k+1}\leq y_k$ can probably still hold. In practice, we find empirically that if α is set to be a small value, the sequence of $\{y_k\}$ is generally decreasing and finally converges to a small value.

Remark 6: Based on the analysis above, the algorithm can be modified to be more efficient in practice. The inner loop of Algorithm 1 has no need to run until convergence. In fact, we can stop the inner loop as long as $f_1(\mathbf{x})-y_kf_2(\mathbf{x})\leq 0$ is satisfied.

V. Monotonic Iterative Method for Spectrum Shaping

In the previous section, we have derived an algorithm named AISS to solve problem (4) and analyzed that the monotonicity of AISS can be guaranteed if $\alpha\to 0$. However, since α is always a nonzero value in practice, the monotonicity has no theoretical guarantee although it usually converges empirically. Thus, we derive another algorithm with the guarantee of strict monotonicity in this section.

A. Minorizer Construction of the Max-Min Problem

Recall that the objective function of problem (16) can be rewritten as follows:

$$\begin{aligned}&\max\left\{\mathbf{x}^H\mathbf{F}_i\mathbf{x}|i\in\mathcal{S}\right\}-y_k\min\left\{\mathbf{x}^H\mathbf{F}_i\mathbf{x}|i\in\mathcal{P}\right\}\\&=-\left(-\max\left\{\mathbf{x}^H\mathbf{F}_i\mathbf{x}|i\in\mathcal{S}\right\}+y_k\min\left\{\mathbf{x}^H\mathbf{F}_i\mathbf{x}|i\in\mathcal{P}\right\}\right)\end{aligned}$$

$$= -\left(\min\left\{-\mathbf{x}^H\mathbf{F}_i\mathbf{x}|i\in\mathcal{S}\right\} + y_k\min\left\{\mathbf{x}^H\mathbf{F}_i\mathbf{x}|i\in\mathcal{P}\right\}\right)$$
$$= -y_k\left(\min\left\{-\frac{1}{y_k}\mathbf{x}^H\mathbf{F}_i\mathbf{x}|i\in\mathcal{S}\right\} + \min\left\{\mathbf{x}^H\mathbf{F}_i\mathbf{x}|i\in\mathcal{P}\right\}\right). \quad (42)$$

Thus, problem (16) is equivalent to

$$\underset{\mathbf{x}\in\mathcal{X}}{\text{maximize}} \quad \min\left\{\mathbf{x}^H\mathbf{F}_i\mathbf{x}|i\in\mathcal{P}\right\} + \min\left\{-y_k\mathbf{x}^H\mathbf{F}_i\mathbf{x}|i\in\mathcal{S}\right\}, \quad (43)$$

where $\widehat{y}_k = \frac{1}{y_k} = \frac{\min\{\mathbf{x}_{k-1}^H\mathbf{F}_i\mathbf{x}_{k-1}|i\in\mathcal{P}\}}{\max\{\mathbf{x}_{k-1}^H\mathbf{F}_i\mathbf{x}_{k-1}|i\in\mathcal{S}\}+c}$.

Furthermore, by introducing an auxiliary variable $\mathbf{p}\in\mathbb{R}^{|\mathcal{S}|}$, we have

$$\min\left\{-\widehat{y}_k\mathbf{x}^H\mathbf{F}_i\mathbf{x}|i\in\mathcal{S}\right\} = \min_{\mathbf{p}\in\mathcal{S}_1}\left\{\sum_{i\in\mathcal{S}} p_i\left(-\widehat{y}_k\mathbf{x}^H\mathbf{F}_i\mathbf{x}\right)\right\} \quad (44)$$

with $\mathcal{S}_1 \triangleq \{\mathbf{p}|\mathbf{1}^T\mathbf{p}=1, \mathbf{p}\geq 0\}$. The optimal $\mathbf{p}$ has only one element being 1 corresponding to the minimal value of $\{\mathbf{x}^H\mathbf{F}_i\mathbf{x}\}_{i=1}^{|\mathcal{P}|}$ and the rest elements are zeros. For the other term, we also have

$$\min\left\{\mathbf{x}^H\mathbf{F}_i\mathbf{x}|i\in\mathcal{P}\right\} = \min_{\mathbf{q}\in\mathcal{S}_2}\left\{\sum_{i\in\mathcal{P}} q_i\mathbf{x}^H\mathbf{F}_i\mathbf{x}\right\}. \quad (45)$$

with $\mathcal{S}_2 \triangleq \left\{\mathbf{q}|\mathbf{1}^T\mathbf{q}=1, \mathbf{q}\geq 0\right\}$. Therefore, problem (43) can be equivalently rewritten as

$$\underset{\mathbf{x}\in\mathcal{X}}{\text{maximize}} \quad \min_{\mathbf{p}\in\mathcal{S}_1,\mathbf{q}\in\mathcal{S}_2}\left\{\sum_{i\in\mathcal{P}} q_i\mathbf{x}^H\mathbf{F}_i\mathbf{x} - \widehat{y}_k\sum_{i\in\mathcal{S}} p_i\mathbf{x}^H\mathbf{F}_i\mathbf{x}\right\}. \quad (46)$$

We will use the MM method to solve problem (46). A minorizer of $\min_{\mathbf{p}\in\mathcal{S}_1,\mathbf{q}\in\mathcal{S}_2}\{\sum_{i\in\mathcal{P}} q_i\mathbf{x}^H\mathbf{F}_i\mathbf{x} - \widehat{y}_k\sum_{i\in\mathcal{S}} p_i\mathbf{x}^H\mathbf{F}_i\mathbf{x}\}$ is provided by the following lemma.

Lemma 7: At the ℓ-th iteration of the MM method, a minorizer of the objective function of problem (46) is given by

$$\ell(\mathbf{x}) = \min_{\mathbf{p}\in\mathcal{S}_1,\mathbf{q}\in\mathcal{S}_2}\left\{\mathrm{Re}\left\{\mathbf{a}_\ell^H\mathbf{x}\right\} + u_\ell(\mathbf{p},\mathbf{q})\right\}, \quad (47)$$

where

$$\mathbf{a}_\ell = 2\left(\sum_{i\in\mathcal{P}} q_j\mathbf{F}_j - \widehat{y}_k\sum_{i\in\mathcal{S}} p_i(\mathbf{F}_i - \mathbf{I})\right)\mathbf{x}_\ell \quad (48)$$

and

$$u_\ell(\mathbf{p},\mathbf{q}) = \widehat{y}_k\sum_{i\in\mathcal{S}} p_i\left(\mathbf{x}_\ell^H\mathbf{F}_i\mathbf{x}_\ell - 2N\right) - \sum_{i\in\mathcal{P}} q_i\mathbf{x}_\ell^H\mathbf{F}_i\mathbf{x}_\ell. \quad (49)$$

Proof: See Appendix C. ■

Therefore, the minorized problem of problem (46) is

$$\begin{aligned}\underset{\mathbf{x}}{\text{maximize}} \quad & \min_{\mathbf{p}\in\mathcal{S}_1,\mathbf{q}\in\mathcal{S}_2}\left\{\mathrm{Re}\left\{\mathbf{a}_\ell^H\mathbf{x}\right\} + u_\ell(\mathbf{p},\mathbf{q})\right\} \\ \text{subject to} \quad & \|\mathbf{x}\|_2^2 = N. \\ & |x_n| \leq \sqrt{\gamma} \ \text{ for } \ n = 1,\ldots,N. \end{aligned} \quad (50)$$

The lemma below converts problem (50) to an equivalent problem, which is relatively easier to solve.

Lemma 8: Solving problem (50) is equivalent to solving the following problem

$$\begin{aligned}\underset{\mathbf{p},\mathbf{q}}{\text{minimize}} \quad & \left(\max_{\|\mathbf{x}\|_2^2\leq N, |x_n|\leq\sqrt{\gamma}} \mathrm{Re}\left\{\mathbf{a}_\ell^H\mathbf{x}\right\}\right) + u_\ell(\mathbf{p},\mathbf{q}) \\ \text{subject to} \quad & \mathbf{p}\in\mathcal{S}_1, \mathbf{q}\in\mathcal{S}_2. \end{aligned} \quad (51)$$

Proof: See Appendix D. ■

Problem (51) can be solved via the projected subgradient method, which finds an ϵ-suboptimal point within a finite number of iterations [38]. Since this method is well established and the application on problem (51) is very straightforward, the details are omitted. In fact, when applying this method, we can stop running the projected subgradient method once it makes $\widehat{y}_{k+1} \geq \widehat{y}_k$, which still guarantees the monotonicity of the whole algorithm.

B. Two Special Cases

1) The Constant Energy Constraint: If $\gamma = N$, then the inner problem of problem (51) becomes

$$\begin{aligned}\underset{\mathbf{x}}{\text{maximize}} \quad & \mathrm{Re}\left\{\mathbf{a}_\ell^H\mathbf{x}\right\} \\ \text{subject to} \quad & \|\mathbf{x}\|_2^2 = N, \end{aligned} \quad (52)$$

which has a closed-form solution given by

$$\mathbf{x}^\star = \frac{\sqrt{N}\mathbf{a}_\ell}{\|\mathbf{a}_\ell\|_2} \quad (53)$$

Substituting (53) back into problem (51), we have

$$\begin{aligned}\underset{\mathbf{p},\mathbf{q}}{\text{minimize}} \quad & \sqrt{N}\|\mathbf{a}_\ell\|_2 + u_\ell(\mathbf{p},\mathbf{q}) \\ \text{subject to} \quad & \mathbf{p}\in\mathcal{S}_1, \mathbf{q}\in\mathcal{S}_2, \end{aligned} \quad (54)$$

which can be rewritten as

$$\begin{aligned}\underset{\mathbf{p},\mathbf{q}}{\text{minimize}} \quad & 2\sqrt{N}\|\mathbf{A}_\ell\mathbf{q} - \mathbf{B}_\ell\mathbf{p}\|_2 - \mathbf{c}_\ell^H\mathbf{q} - \mathbf{d}_\ell^H\mathbf{p} \\ \text{subject to} \quad & \mathbf{p}\in\mathcal{S}_1, \mathbf{q}\in\mathcal{S}_2. \end{aligned} \quad (55)$$

where

$$\mathbf{A}_\ell = \left[\mathbf{F}_1\mathbf{x}_\ell, \mathbf{F}_2\mathbf{x}_\ell, \ldots, \mathbf{F}_{|\mathcal{P}|}\mathbf{x}_\ell\right], \quad (56)$$

$$\mathbf{B}_\ell = \left[y_k\mathbf{F}_1\mathbf{x}_\ell - y_k\mathbf{x}_\ell, \ldots, y_k\mathbf{F}_{|\mathcal{S}|}\mathbf{x}_\ell - \mathbf{x}_\ell\right], \quad (57)$$

$$\mathbf{c}_\ell = \left[\mathbf{x}_\ell^H\mathbf{F}_1\mathbf{x}_\ell, \ldots, \mathbf{x}_\ell^H\mathbf{F}_{|\mathcal{P}|}\mathbf{x}_\ell\right]^T, \quad (58)$$

$$\mathbf{d}_\ell = \begin{bmatrix} \widehat{y}_k\left(2N - \mathbf{x}_\ell^H\mathbf{F}_1\mathbf{x}_\ell\right) \\ \vdots \\ \widehat{y}_k\left(2N - \mathbf{x}_\ell^H\mathbf{F}_{|\mathcal{S}|}\mathbf{x}_\ell\right) \end{bmatrix}. \quad (59)$$

Problem (55) can be rewritten in a second-order cone programming (SOCP) form and solved efficiently by any off-the-shelf solver like SeDuMi, SDPT3 or Mosek.

2) The Unit-Modulus Constraint: If $\gamma = 1$, then the inner problem of problem (51) becomes

$$\begin{aligned} \underset{\mathbf{x}}{\text{maximize}} \quad & \text{Re}\left\{\mathbf{a}_\ell^H \mathbf{x}\right\} \\ \text{subject to} \quad & |x_n| = 1 \ \text{ for } \ n = 1, \ldots, N. \end{aligned} \tag{60}$$

which has a closed-form solution given by

$$\mathbf{x}^\star = e^{j\text{arg}(\mathbf{a}_\ell)} \tag{61}$$

with $e^{j\text{arg}(\cdot)}$ being an elementwise operation. Substituting (61) back into problem (51), we have

$$\begin{aligned} \underset{\mathbf{p},\mathbf{q}}{\text{minimize}} \quad & \|\mathbf{a}_\ell\|_1 + u_\ell\left(\mathbf{p}, \mathbf{q}\right) \\ \text{subject to} \quad & \mathbf{p} \in \mathcal{S}_1, \mathbf{q} \in \mathcal{S}_2, \end{aligned}$$

which can also be rewritten as

$$\begin{aligned} \underset{\mathbf{p},\mathbf{q}}{\text{minimize}} \quad & 2\left\|\mathbf{A}_\ell \mathbf{q} - \mathbf{B}_\ell \mathbf{p}\right\|_1 - \mathbf{c}_\ell^H \mathbf{q} - \mathbf{d}_\ell^H \mathbf{p} \\ \text{subject to} \quad & \mathbf{p} \in \mathcal{S}_1, \mathbf{q} \in \mathcal{S}_2. \end{aligned} \tag{62}$$

Problem (62) is convex and can be solved efficiently by solvers.

C. Complexity and Convergence Analysis

The DFT matrix is decomposed into two submatrices: the passband DFT matrix $\mathbf{F}_\mathcal{P} = [\mathbf{f}_1, \ldots, \mathbf{f}_{|\mathcal{P}|}]$ and the stopband DFT matrix $\mathbf{F}_\mathcal{S} = [\mathbf{f}_1, \ldots, \mathbf{f}_{|S|}]$. The complete description of the proposed algorithm, named as **M**onotonic **I**terative Method for **S**pectrum **S**haping (MISS), is given in Algorithm 2.

From the pseudo code of the proposed MISS, the main computations include $\mathbf{F}_\mathcal{P}^H \mathbf{x}_\ell$, $\mathbf{F}_\mathcal{S}^H \mathbf{x}_\ell$ and solving problem (55) or (62). The first four computations can be implemented via fast Fourier transform and thus require $\mathcal{O}(NlogN)$ flops. Assume that both problem (55) and (62) are solved by the solver CVX, which will adopts a primal-dual interior point method with the worst-case computational complexity being $\mathcal{O}(N^{3.5})$. Therefore, in the worst case, the complexity of each iteration of MISS is $\mathcal{O}(N^{3.5})$. As illustrated in the preliminary part, both the Dinkelbach's algorithm and the MM method can guarantee the monotonicity. Thus, the monotonicity of the proposed MISS can be guaranteed. Note that the monotonicity of the outer Dinkelbach's algorithm is still guaranteed as long as $f_1(\mathbf{x}) - \widehat{y}_k f_2(\mathbf{x}) \leq 0$, which means that the inner MM method can be run for only several or even one iteration.

Algorithm 2: The Monotonic Iterative Method for Spectrum Shaping (MISS).

Require: The stopband $\mathcal{S}$ and passband $\mathcal{P}$.

Set $k = 0$, initialize $\mathbf{x}_0$
Repeat
  $\widehat{y}_k = \frac{\max\left\{\mathbf{x}_k^H \mathbf{F}_i \mathbf{x}_k | i \in \mathcal{S}\right\}}{\min\left\{\mathbf{x}_k^H \mathbf{F}_i \mathbf{x}_k | i \in \mathcal{P}\right\} + c}$
  Set $\ell = 0$, $\mathbf{s}_\ell = \mathbf{x}_k$
  Repeat
    $\mathbf{A}_\ell = \mathbf{F}_\mathcal{P} \text{Diag}\left(\mathbf{F}_\mathcal{P}^H \mathbf{s}_\ell\right)$
    $\mathbf{B}_\ell = \widehat{y}_k \left(\mathbf{F}_S \text{Diag}\left(\mathbf{F}_\mathcal{S}^H \mathbf{s}_\ell\right) - \mathbf{1}_{|\mathcal{S}|}^T \otimes \mathbf{s}_\ell\right)$
    $\mathbf{c}_\ell = \left[\text{abs}\left(\mathbf{F}_\mathcal{P}^H \mathbf{s}_\ell\right)\right]^2$
    $\mathbf{d}_\ell = \widehat{y}_k \left(2N\mathbf{1} - \left[\text{abs}\left(\mathbf{F}_\mathcal{S}^H \mathbf{s}_\ell\right)\right]^2\right)$
    Obtain $(\mathbf{p}_{\ell+1}, \mathbf{q}_{\ell+1})$ by solving problem (55) or (62)
    $\mathbf{a}_{\ell+1} = 2\left(\mathbf{A}_\ell \mathbf{q}_{\ell+1} - \mathbf{B}_\ell \mathbf{p}_{\ell+1}\right)$
    $\mathbf{s}_{\ell+1} = \frac{\sqrt{N}\mathbf{a}_{\ell+1}}{\|\mathbf{a}_{\ell+1}\|_2}$ $(\mathbf{s}_{\ell+1} = e^{j\text{arg}(\mathbf{a}_{\ell+1})})$
    $\ell \leftarrow \ell + 1$
  Until convergence
  $\mathbf{x}_{k+1} = \mathbf{s}_\ell$
  $k \leftarrow k + 1$
Until convergence

VI. Numerical Experiments

In this section, we conduct numerical experiments to evaluate the performance of the two proposed methods and compare them with the existing benchmark. Assume that the transmitted sequence has the length $N = 162$. This sequence is transmitted in multiple electromagnetic service environment, where the stopbands are given by

$$\begin{aligned} \mathcal{S} = \ & [0, 0.0617] \cup [0.0988, 0.2469] \cup [0.2593, 0.2840] \\ & \cup [0.3086, 0.3827] \cup [0.4074, 0.4938] \\ & \cup [0.5185, 0.5558] \cup [0.9383, 1], \end{aligned} \tag{63}$$

where the frequency is normalized so that the total range is $[0, 1]$. The passbands consist of the complementary sets of $\mathcal{S}$ within $[0, 1]$. The benchmark method for this design problem is the NSLM (No-Spectral-Level-Mask) method [27], which is for the unit modulus case. The parameter settings of NSLM follow the suggestions of [27]. Unless otherwise specified, all the parameters are the same in the numerical experiments. All experiments were carried out on a Window desktop PC with a 3.30 GHz i5-4950 CPU and 8 GB RAM.

A. Convergence Performance and Shaped Spectrum

Note that the proposed MISS has the guarantee of monotonicity. Figure 2 shows the convergence plot of MISS for the two special cases $\gamma = 1$ and $\gamma = N$ for the first 20 s. In fact, all AISS curves will achieve around 1.5×10^{-7} after running for 300 s, while the (A)NSLM curve barely decreases after the first 20 s. We can see clearly that MISS can guarantee the monotonicity strictly but at at the cost of high computational complexity. Considering that neither of the proposed AISS and the benchmark NSLM has this monotonicity guarantee, a good usage of MISS is to provide good initialization for AISS and NSLM.

Figure 3 shows the curves of the SLR along the CPU time, where the initial point for AISS and NSLM is provided by MISS after a few iterations. From the figure, we can see clearly that AISS decreases much faster and achieves better SLR than NSLM. In addition, although neither AISS nor NSLM has monotonicity guarantee, both can still decrease the objective value along iterations generally. In fact, by choosing a small α, we can reasonably expect that AISS performs well with only small fluctuations or even no fluctuation. The spectra of the

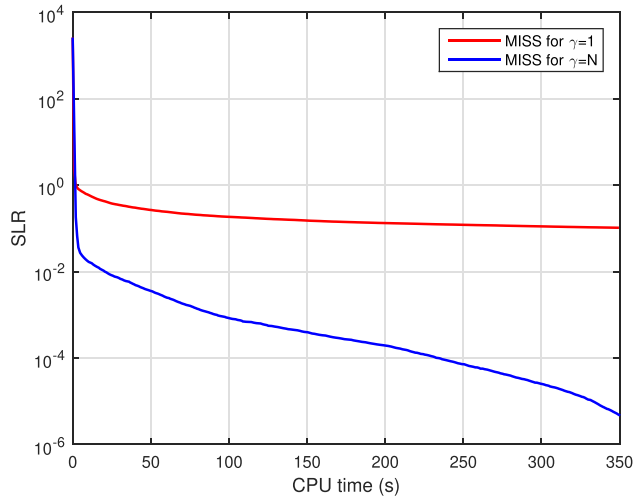

Fig. 2. Convergence plot of objective value versus CPU time of MISS.

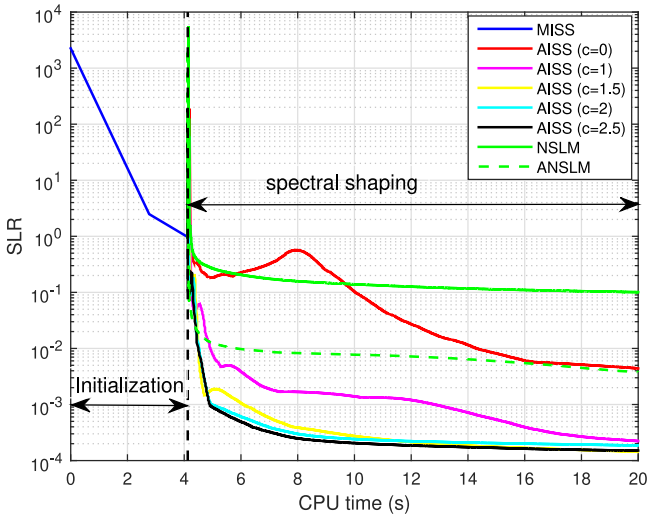

Fig. 3. Convergence plot of objective value versus CPU time for $\gamma = 1$ and $\alpha = 1 \times 10^{-10}$.

designed sequences are shown in Figure 4. The AISS can shape deep notches in these stopbands.

Table I shows the comparison of average performance between AISS and NSLM. For each value of N, we conduct 50 random trails. In both columns of SLR and CPU time, each presented value is the average of the 50 outcomes. In the last column named exhaustion, the value represents the percentage of occurrence of the algorithm stopped by meeting the maximum number of iterations. Note that the stopping criterion for both AISS and MISS is $(\|\mathbf{x}_{k+1} - \mathbf{x}_k\|_2 / \|\mathbf{x}_k\|_2 \leq \varepsilon$ or $k \geq K)$, where $\varepsilon = 1 \times 10^{-8}, K = 5 \times 10^3$ for AISS and $\varepsilon = 1 \times 10^{-8}$, $K = 5 \times 10^4$ for NSLM. From Table I, we can see that AISS is better than NSLM in terms of both CPU time and SLR (only except the case $N = 50$).

B. Parameter Effect on the Performance of AISS

Compared with MISS and NSLM, AISS can deal with the general PAR constraint. Figure 5 shows the effect of different

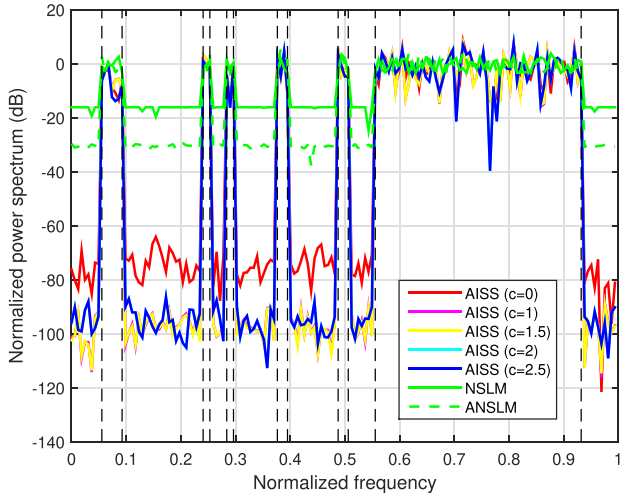

Fig. 4. Comparison of the spectra of the designed sequences for $\gamma = 1$ and $\alpha = 1 \times 10^{-10}$.

TABLE I
PERFORMANCE EVALUATION OF AISS AND NSLM

Length	Method	SLR (dB)	CPU time (s)	Exhaustion
$N = 50$	AISS	-2.8243	**14.1050**	76.67%
	NSLM	**-8.8741**	34.4193	100.00%
$N = 100$	AISS	**-11.2808**	**36.7730**	86.67%
	NSLM	-4.4524	66.5400	100.00%
$N = 150$	AISS	**-16.7633**	**67.4600**	100.00%
	NSLM	-0.3881	115.6813	100.00%
$N = 200$	AISS	**-17.9391**	**117.7323**	100.00%
	NSLM	0.1919	179.1473	100.00%
$N = 250$	AISS	**-22.2534**	**160.5987**	100.00%
	NSLM	6.9316	250.7623	100.00%
$N = 300$	AISS	**-16.2970**	**240.3300**	100.00%
	NSLM	8.9960	370.6253	100.00%

value of γ on the SLR performance, where 50 random trials are conducted for each γ. From this figure, we can see that the objective value is generally decreasing as the value of γ increases. From the perspective of optimization, it is reasonable because as γ increases, the feasible set extends so that the achieved objective value probably becomes smaller and smaller. However, the improvement of the averaged objective value is very significant when γ is changed from 1 to 2. After 6, the averaged objective value does not decrease too much.

In Figure 6, we show the spectra of the designed sequence for different values of γ, where the AISS uses an randomly generated initial sequence. It is clear to see that there are notches in the stopands and these notches becomes deeper when the value of γ increases. But for the cases $\gamma = 5$ and $\gamma = 7$, the spectra are generally the same, which is consistent to the information provided by Figure 5.

As illustrated above, an important issue of using AISS is the choice of α, which controls the degree of approximation. The sensitivity of AISS on the choice of α is shown in Figure 7, where 50 random trials are conducted. Fortunately, the performance is not too sensitive to that choice. We can also see that the achieved average objective values are around 10^{-3} when α is within $[1 \times 10^{-8}, 1 \times 10^{-6}]$.

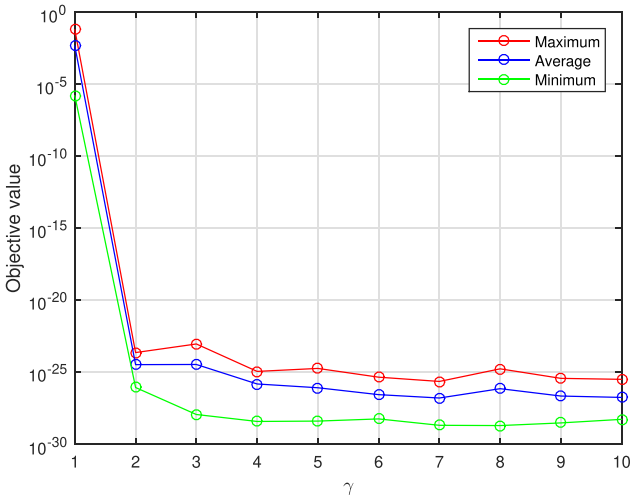

Fig. 5. Effect of different γ on the objective value for AISS over 50 trials.

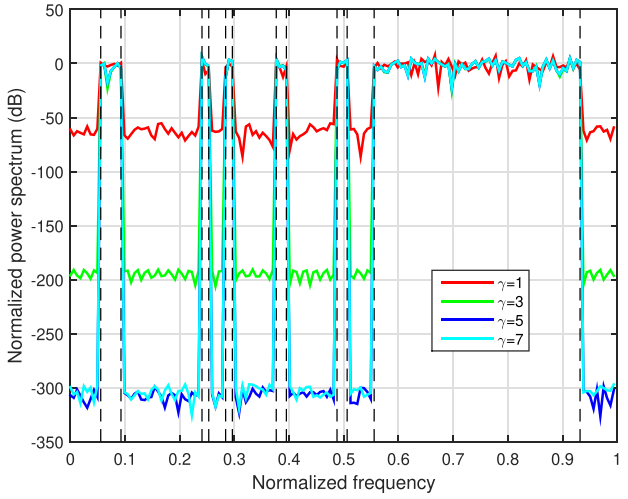

Fig. 6. Comparison of spectra for different PAR levels of AISS. $\alpha = 1 \times 10^{-7}$.

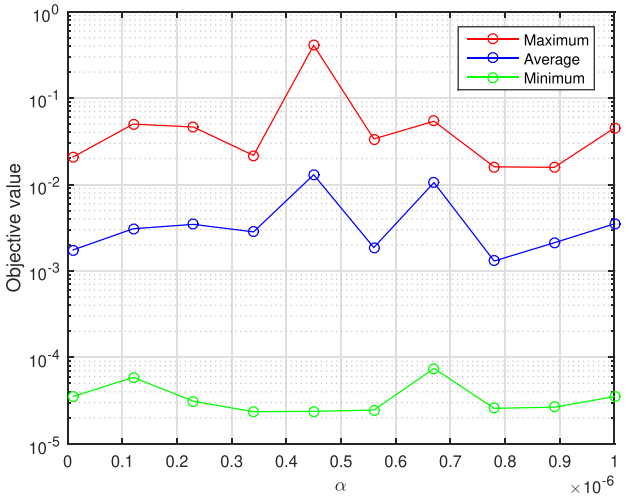

Fig. 7. Sensitivity of AISS on the choice of α for $\gamma = 1$.

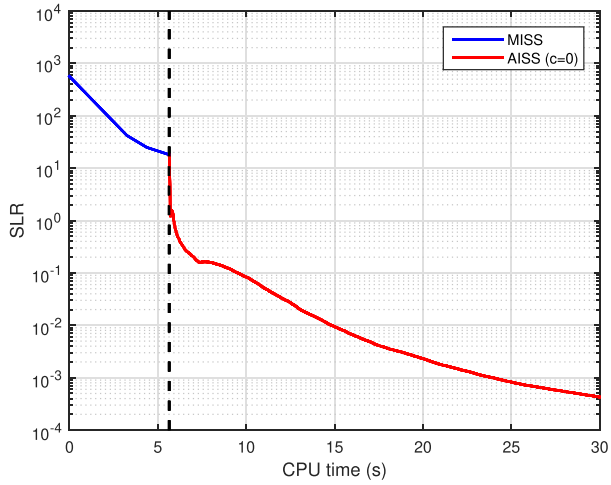

(a) Convergence plot of objective value versus CPU time for γ= 1.

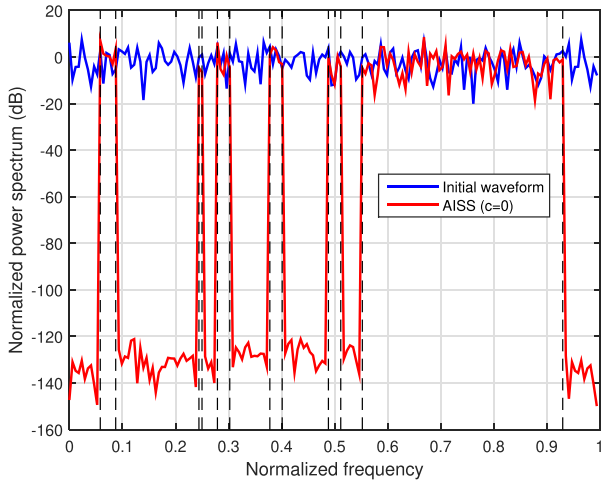

(b) Comparison of spectra for initial waveform and designed waveform.

Fig. 8. The frequency oversampling case: sequence length: $N = 162$; number of frequency points: $M = N + 10$.

C. Proposed Methods for Frequency Oversampling

As we illustrated previously, if frequency oversampling (more than N frequency samples) is considered for the passbands and stopbands, then the SLR is suitable for optimization which is the RSLR with $c = 0$. The proposed AISS and MISS based on the RSLR can be applied to the frequency oversampling case, of which the simulation resluts are shown in Figure 8. Note that for the convergence plot, we only show the first 30 seconds to demonstrate the fluctuation of AISS. The red curve will finally converge to SLR $= 5.5514 \times 10^{-11}$ at CPU time $= 189.5469$.

VII. Conclusion

In this paper, the sequence design problem for spectral shaping is considered, which is formulated as the minimization of the regularized SLR subject to the PAR and constant energy constraints. We have derived two algorithms named AISS and MISS,

respectively. Both algorithms are based on the combination of the Dinkelbach's algorithm and the MM method, and the difference between them is that AISS approximates the iterative subproblem of the Dinkelbach's framework while MISS solve that directly. Consequently, the AISS has a lower computational complexity but has no strict guarantee of monotonicity, while the MISS is on the contrary. In order to make the best of each algorithm, a suggested implementation is to use MISS generate a good initialization, and then use AISS to shape the spectrum based on this initialization. In the numerical experiments, the combination of MISS and AISS is verified and AISS shows better performance than the benchmark in terms of both SLR and running time.

APPENDIX

A. Proof of Lemma 1

Proof: According to the log-sum-exp approximation [39],

$$\begin{aligned}\max\left\{\frac{\mathbf{x}^H\mathbf{F}_i\mathbf{x}}{\alpha}|i\in\mathcal{S}\right\} &\le \log\sum_{i\in\mathcal{S}}\exp\left(\frac{\mathbf{x}^H\mathbf{F}_i\mathbf{x}}{\alpha}\right)\\ &\le \log|\mathcal{S}|+\max\left\{\frac{\mathbf{x}^H\mathbf{F}_i\mathbf{x}}{\alpha}|i\in\mathcal{S}\right\}.\end{aligned} \tag{64}$$

which is further equivalent to

$$\begin{aligned}\max\left\{\mathbf{x}^H\mathbf{F}_i\mathbf{x}|i\in\mathcal{S}\right\} &\le \alpha\log\sum_{i\in\mathcal{S}}\exp\left(\frac{\mathbf{x}^H\mathbf{F}_i\mathbf{x}}{\alpha}\right)\\ &\le \alpha\log|\mathcal{S}|+\max\left\{\mathbf{x}^H\mathbf{F}_i\mathbf{x}|i\in\mathcal{S}\right\}.\end{aligned} \tag{65}$$

Similarly, for the term $\max\{-\mathbf{x}^H\mathbf{F}_j\mathbf{x}|j\in\mathcal{P}\}$, we have

$$\begin{aligned}\max\left\{-\mathbf{x}^H\mathbf{F}_j\mathbf{x}|j\in\mathcal{P}\right\} &\le \alpha\log\sum_{j\in\mathcal{P}}\exp\left(-\frac{\mathbf{x}^H\mathbf{F}_j\mathbf{x}}{\alpha}\right)\\ &\le \alpha\log|\mathcal{P}|+\max\left\{-\mathbf{x}^H\mathbf{F}_j\mathbf{x}|j\in\mathcal{P}\right\}.\end{aligned} \tag{66}$$

Thus, the objective function of problem (17) can be approximated by $\alpha\log\sum_{i\in\mathcal{S}}\exp(\frac{\mathbf{x}^H\mathbf{F}_i\mathbf{x}}{\alpha})+\alpha y_k\log\sum_{j\in\mathcal{P}}\exp(-\frac{\mathbf{x}^H\mathbf{F}_j\mathbf{x}}{\alpha})$, and the approximation error is at most $\alpha(\log|\mathcal{S}|+y_k\log|\mathcal{P}|)$. ■

B. Proof of Lemma 2

Proof: At the ℓ-th iteration of the MM method, by using the concavity of logarithm, we have

$$\begin{aligned}&\log\sum_{i\in\mathcal{S}}\exp\left(-\mathbf{x}^H\tilde{\mathbf{F}}_i\mathbf{x}\right)\\ &\le \frac{\sum_{i\in\mathcal{S}}\exp\left(-\mathbf{x}^H\tilde{\mathbf{F}}_i\mathbf{x}\right)}{\sum_{i\in\mathcal{S}}\exp\left(-\mathbf{x}_\ell^H\tilde{\mathbf{F}}_i\mathbf{x}_\ell\right)}+\log\sum_{i\in\mathcal{S}}\exp\left(-\mathbf{x}_\ell^H\tilde{\mathbf{F}}_i\mathbf{x}_\ell\right)-1\end{aligned} \tag{67}$$

with the equality achieved when $\mathbf{x}=\mathbf{x}_\ell$.

The function $f(x)=e^{-x}, x\in(0,+\infty)$ is β-smooth (i.e., the derivative of $f(x)$ is is Lipschitz continuous) with $\beta=1$ because $|f''(x)|=e^{-x}<1$ for $x\in(0,+\infty)$. Thus, for $x,y\in(0,+\infty)$, $f(x)$ is upper bounded by a quadratic function given by

$$f(x)\le f(y)+\nabla f(y)^T(x-y)+\frac{1}{2}||x-y||^2 \tag{68}$$

with the equality achieved when $x=y$. Substituting $x=\mathbf{x}^H\tilde{\mathbf{F}}_i\mathbf{x}$ and $y=\mathbf{x}_\ell^H\tilde{\mathbf{F}}_i\mathbf{x}_\ell$ into (68), we have

$$\begin{aligned}&\exp\left(-\mathbf{x}^H\tilde{\mathbf{F}}_i\mathbf{x}\right)\\ &\le \exp\left(-\mathbf{x}_\ell^H\tilde{\mathbf{F}}_i\mathbf{x}_\ell\right)-\exp\left(-\mathbf{x}_\ell^H\tilde{\mathbf{F}}_i\mathbf{x}_\ell\right)\left(\mathbf{x}^H\tilde{\mathbf{F}}_i\mathbf{x}-\mathbf{x}_\ell^H\tilde{\mathbf{F}}_i\mathbf{x}_\ell\right)\\ &\quad+\frac{1}{2}\left\|\mathbf{x}^H\tilde{\mathbf{F}}_i\mathbf{x}-\mathbf{x}_\ell^H\tilde{\mathbf{F}}_i\mathbf{x}_\ell\right\|_2^2\\ &=\frac{1}{2}\mathbf{x}^H\tilde{\mathbf{F}}_i^H\mathbf{x}\mathbf{x}^H\tilde{\mathbf{F}}_i\mathbf{x}-\left(\mathbf{x}_\ell^H\tilde{\mathbf{F}}_i^H\mathbf{x}_\ell+\exp\left(-\mathbf{x}_\ell^H\tilde{\mathbf{F}}_i\mathbf{x}_\ell\right)\right)\mathbf{x}^H\tilde{\mathbf{F}}_i\mathbf{x}\\ &\quad+\text{constant}\end{aligned} \tag{69}$$

with the equality achieved when $\mathbf{x}=\mathbf{x}_\ell$.

By combining (67) and (69), $\log\sum_{i\in\mathcal{S}}\exp(-\mathbf{x}^H\tilde{\mathbf{F}}_i\mathbf{x})$ can be majorized as

$$\begin{aligned}&\log\sum_{i\in\mathcal{S}}\exp\left(-\mathbf{x}^H\tilde{\mathbf{F}}_i\mathbf{x}\right)\\ &\le\sum_{i\in\mathcal{S}}\left(\frac{1}{2a^\ell}\mathbf{x}^H\tilde{\mathbf{F}}_i^H\mathbf{x}\mathbf{x}^H\tilde{\mathbf{F}}_i\mathbf{x}-\frac{b_i^\ell}{a^\ell}\mathbf{x}^H\tilde{\mathbf{F}}_i\mathbf{x}\right)+\text{constant},\end{aligned} \tag{70}$$

where

$$a^\ell=\sum_{i\in\mathcal{S}}\exp\left(-\mathbf{x}_\ell^H\tilde{\mathbf{F}}_i\mathbf{x}_\ell\right)>0, \tag{71}$$

$$b_i^\ell=\mathbf{x}_\ell^H\tilde{\mathbf{F}}_i^H\mathbf{x}_\ell+\exp\left(-\mathbf{x}_\ell^H\tilde{\mathbf{F}}_i\mathbf{x}_\ell\right)>0. \tag{72}$$

Next, the majorizer of $\frac{1}{2a^\ell}\mathbf{x}^H\tilde{\mathbf{F}}_i^H\mathbf{x}\mathbf{x}^H\tilde{\mathbf{F}}_i\mathbf{x}-\frac{b_i^\ell}{a^\ell}\mathbf{x}^H\tilde{\mathbf{F}}_i\mathbf{x}$ will be constructed. Let $\mathbf{X}=\mathbf{x}\mathbf{x}^H$, then $\mathbf{x}^H\tilde{\mathbf{F}}_i^H\mathbf{x}\mathbf{x}^H\tilde{\mathbf{F}}_i\mathbf{x}=\text{vec}(\mathbf{x})^H\text{vec}(\tilde{\mathbf{F}}_i)\text{vec}(\tilde{\mathbf{F}}_i)^H\text{vec}(\mathbf{x})$. The largest eigenvalue of $\bar{\mathbf{F}}_i=\text{vec}(\tilde{\mathbf{F}}_i)\text{vec}(\tilde{\mathbf{F}}_i)^H$ is

$$\begin{aligned}\lambda_{max}\left(\bar{\mathbf{F}}_i\right)&=\text{vec}\left(\tilde{\mathbf{F}}_i\right)^H\text{vec}\left(\tilde{\mathbf{F}}_i\right)\\ &=\frac{1}{\alpha^2}\text{tr}\left(\left((1+\epsilon)\mathbf{I}-\mathbf{F}_i\right)^H\left((1+\epsilon)\mathbf{I}-\mathbf{F}_i\right)\right)\\ &=\frac{1}{\alpha^2}\left((1+\epsilon)^2N-2(1+\epsilon)+1\right)\end{aligned} \tag{73}$$

According to [25, Lemma 1], we have

$$\begin{aligned}&\mathbf{x}^H\tilde{\mathbf{F}}_i^H\mathbf{x}\mathbf{x}^H\tilde{\mathbf{F}}_i\mathbf{x}\\ &=\text{vec}(\mathbf{x})^H\text{vec}\left(\tilde{\mathbf{F}}_i\right)\text{vec}\left(\tilde{\mathbf{F}}_i\right)^H\text{vec}(\mathbf{x})\\ &\le 2\text{Re}\left(\text{vec}\left(\mathbf{X}_\ell\right)^H\left(\bar{\mathbf{F}}_i-\lambda_{max}\left(\bar{\mathbf{F}}_i\right)\mathbf{I}\right)\text{vec}(\mathbf{x})\right)+\text{constant}\\ &=2\text{Re}\left[\mathbf{x}^H\left(\text{tr}\left(\mathbf{X}_\ell\tilde{\mathbf{F}}_i\right)\tilde{\mathbf{F}}_i-\lambda_{max}\left(\bar{\mathbf{F}}_i\right)\mathbf{X}_\ell\right)\mathbf{x}\right]+\text{constant}\\ &=2\mathbf{x}^H\left(\mathbf{x}_\ell^H\tilde{\mathbf{F}}_i\mathbf{x}_\ell\tilde{\mathbf{F}}_i-\lambda_{max}\left(\bar{\mathbf{F}}_i\right)\mathbf{X}_\ell\right)\mathbf{x}+\text{constant}.\end{aligned} \tag{74}$$

Thus, we have

$$\frac{1}{2a^\ell}\mathbf{x}^H\tilde{\mathbf{F}}_i^H\mathbf{x}\mathbf{x}^H\tilde{\mathbf{F}}_i\mathbf{x} - \frac{b_i^\ell}{a^\ell}\mathbf{x}^H\tilde{\mathbf{F}}_i\mathbf{x} \le \mathbf{x}^H\mathbf{A}_i^\ell\mathbf{x} + \text{constant}, \tag{75}$$

where $\mathbf{A}_i^\ell$ is defined by (24). Due to $\mathbf{A}_i^\ell \preceq \mathbf{0}$, the concave term $\mathbf{x}^H\mathbf{A}_i^\ell\mathbf{x}$ can be further majorized by its first-order Taylor expansion given by

$$\mathbf{x}^H\mathbf{A}_i^\ell\mathbf{x} \le 2\text{Re}\left(\mathbf{x}_\ell^H\mathbf{A}_i^\ell\mathbf{x}\right) + \text{constant}. \tag{76}$$

We have

$$\frac{\mathbf{x}^H\tilde{\mathbf{F}}_i^H\mathbf{x}\mathbf{x}^H\tilde{\mathbf{F}}_i\mathbf{x}}{2a^\ell} - \frac{b_i^\ell}{a^\ell}\mathbf{x}^H\tilde{\mathbf{F}}_i\mathbf{x} \le 2\text{Re}\left(\mathbf{x}_\ell^H\mathbf{A}_i^\ell\mathbf{x}\right) + \text{constant}, \tag{77}$$

Therefore, by combining (70) and (77), we have

$$\log\sum_{i\in\mathcal{S}}\exp\left(-\mathbf{x}^H\tilde{\mathbf{F}}_i\mathbf{x}\right) \le 2\text{Re}\left[\left(\sum_{i\in\mathcal{S}}\mathbf{A}_i^\ell\mathbf{x}_\ell\right)^H\mathbf{x}\right] + \text{constant}.$$

■

C. Proof of Lemma 7

Proof: Define $f_1(\mathbf{x}) = \sum_{j\in\mathcal{P}} q_j\mathbf{x}^H\mathbf{F}_j\mathbf{x}$ and $f_2(\mathbf{x}) = \sum_{i\in\mathcal{S}} p_i\mathbf{x}^H\mathbf{F}_i\mathbf{x}$. The convex function $f_1(\mathbf{x})$ can be lower bounded by its first-order Taylor expansion as follows

$$\sum_{j\in\mathcal{P}} q_j\mathbf{x}^H\mathbf{F}_j\mathbf{x} \ge \sum_{j\in\mathcal{P}} q_j\left[\mathbf{x}_\ell^H\mathbf{F}_j\mathbf{x}_\ell + 2\text{Re}\left(\mathbf{x}_\ell^H\mathbf{F}_j\left(\mathbf{x}-\mathbf{x}_\ell\right)\right)\right]. \tag{78}$$

According to [25, Lemma 1], for each $i \in \mathcal{S}$, we have

$$\mathbf{x}^H\mathbf{F}_i\mathbf{x} \le \mathbf{x}^H\mathbf{x} + 2\text{Re}\left(\mathbf{x}_\ell^H\left(\mathbf{F}_i-\mathbf{I}\right)\mathbf{x}\right) + \mathbf{x}_\ell^H\left(\mathbf{I}-\mathbf{F}_i\right)\mathbf{x}_\ell, \tag{79}$$

where $\lambda_u(\mathbf{F}_i)$ is an upper bound of the eigenvalues of $\mathbf{F}_i$.

Thus, by combining (78) and (79) and doing some algebra manipulations, we have

$$\begin{aligned}
&\sum_{j\in\mathcal{P}} q_j\mathbf{x}^H\mathbf{F}_j\mathbf{x} - y_k\sum_{i\in\mathcal{S}} p_i\mathbf{x}^H\mathbf{F}_i\mathbf{x} \\
&\ge \text{Re}\left[\mathbf{x}_\ell^H\left(\sum_{j\in\mathcal{P}} 2q_j\mathbf{F}_j - y_k\sum_{i\in\mathcal{S}} 2p_i\left(\mathbf{F}_i-\mathbf{I}\right)\right)^H\mathbf{x}\right] \\
&\quad - y_k\sum_{i\in\mathcal{S}} p_i\left(N + \mathbf{x}_\ell^H\left(\mathbf{I}-\mathbf{F}_i\right)\mathbf{x}_\ell\right) - \sum_{j\in\mathcal{P}} q_j\mathbf{x}_\ell^H\mathbf{F}_j\mathbf{x}_\ell.
\end{aligned} \tag{80}$$

Define $\mathbf{a}_\ell$ and $u_\ell(\mathbf{p},\mathbf{q})$ as (48) and (49), then we have

$$\begin{aligned}
&\min_{\mathbf{p}\in\mathcal{S}_1,\mathbf{q}\in\mathcal{S}_2}\left\{\sum_{j\in\mathcal{P}} q_j\mathbf{x}^H\mathbf{F}_j\mathbf{x} - y_k\sum_{i\in\mathcal{S}} p_i\mathbf{x}^H\mathbf{F}_i\mathbf{x}\right\} \\
&\quad\ge \min_{\mathbf{p}\in\mathcal{S}_1,\mathbf{q}\in\mathcal{S}_2}\left\{\text{Re}\left\{\mathbf{a}_\ell^H\mathbf{x}\right\} + u_\ell\left(\mathbf{p},\mathbf{q}\right)\right\}
\end{aligned} \tag{81}$$

with equality achieved when $\mathbf{x} = \mathbf{x}_\ell$. ■

D. Proof of Lemma 8

Proof: First, problem (50) is equivalent to

$$\begin{aligned}
\underset{\mathbf{x}}{\text{maximize}} \quad & \min_{\mathbf{p}\in\mathcal{S}_1,\mathbf{q}\in\mathcal{S}_2}\left\{\text{Re}\left\{\mathbf{a}_\ell^H\mathbf{x}\right\} + u_\ell\left(\mathbf{p},\mathbf{q}\right)\right\} \\
\text{subject to} \quad & \|\mathbf{x}\|_2^2 \le N. \\
& |x_n| \le \sqrt{\gamma} \ \text{ for } \ n = 1,\ldots,N.
\end{aligned} \tag{82}$$

The optimal solution to problem (82) should satisfy $\|\mathbf{x}^\star\|_2^2 = N$. Otherwise, we can always scale up some elements of $\mathbf{x}^\star$ with a larger objective value.

For problem (82), the objective function is bilinear in $\mathbf{x}$ and $(\mathbf{p},\mathbf{q})$, and the constraint sets for $\mathbf{x}$ and $(\mathbf{p},\mathbf{q})$ are both compact convex. According to the minimax theorem [40]–[42], the equality is achieved so that max and min can be exchanged. Thus, we have the following equivalent problem

$$\begin{aligned}
\underset{\mathbf{p},\mathbf{q}}{\text{minimize}} \quad & \left(\max_{\|\mathbf{x}\|_2^2\le N,|x_n|\le\sqrt{\gamma}} \text{Re}\left\{\mathbf{a}_\ell^H\mathbf{x}\right\}\right) + u_\ell\left(\mathbf{p},\mathbf{q}\right) \\
\text{subject to} \quad & \mathbf{p}\in\mathcal{S}_1, \mathbf{q}\in\mathcal{S}_2.
\end{aligned} \tag{83}$$

■

REFERENCES

[1] H. He, J. Li, and P. Stoica, *Waveform Design for Active Sensing Systems: A Computational Approach*. Cambridge, U.K.: Cambridge Univ. Press, 2012.

[2] J. Li and P. Stoica, *MIMO Radar Signal Processing*. Hoboken, NJ, USA: Wiley, 2008.

[3] J. Liang, L. Xu, J. Li, and P. Stoica, "On designing the transmission and reception of multistatic continuous active sonar systems," *IEEE Trans. Aerosp. Electron. Syst.*, vol. 50, no. 1, pp. 285–299, Jan. 2014.

[4] M. Labib, V. Marojevic, A. F. Martone, J. H. Reed, and A. I. Zaghloul, "Coexistence between communication and radar systems-a survey," URSI, vol. 2017, no. 362, pp. 74–82, 2017.

[5] M. Wicks, "Spectrum crowding and cognitive radar," in *Proc. IEEE 2nd Int. Workshop Cogn. Inf. Process.*, 2010, pp. 452–457.

[6] M. E. Davis, "Frequency allocation challenges for ultra-wideband radars," in *Proc. IET Int. Conf. Radar Syst.*, IEEE, vol. 28, no. 7, 2013, pp. 12–18.

[7] G. Wang and Y. Lu, "Designing single/multiple sparse frequency waveforms with sidelobe constraint," *IET Radar, Sonar Navigation*, vol. 5, no. 1, pp. 32–38, 2011.

[8] A. Aubry, V. Carotenuto, A. De Maio, A. Farina, and L. Pallotta, "Optimization theory-based radar waveform design for spectrally dense environments," *IEEE Aerosp. Electron. Syst. Mag.*, vol. 31, no. 12, pp. 14–25, Dec. 2016.

[9] G. Cui, X. Yu, G. Foglia, Y. Huang, and J. Li, "Quadratic optimization with similarity constraint for unimodular sequence synthesis," *IEEE Trans. Signal Process.*, vol. 65, no. 18, pp. 4756–4769, Sep. 2017.

[10] J. Li, J. R. Guerci, and L. Xu, "Signal waveform's optimal under restriction design for active sensing," in *Proc. 4th IEEE Workshop Sensor Array Multichannel Process.*, 2006, pp. 382–386.

[11] M. J. Lindenfeld, "Sparse frequency transmit-and-receive waveform design," *IEEE Trans. Aerosp. Electron. Syst.*, vol. 40, no. 3, pp. 851–861, Jul. 2004.

[12] A. Aubry, A. De Maio, M. Piezzo, and A. Farina, "Radar waveform design in a spectrally crowded environment via nonconvex quadratic optimization," *IEEE Trans. Aerosp. Electron. Systems*, vol. 50, no. 2, pp. 1138–1152, Apr. 2014.

[13] A. Aubry, A. De Maio, Y. Huang, M. Piezzo, and A. Farina, "A new radar waveform design algorithm with improved feasibility for spectral coexistence," *IEEE Trans. Aerosp. Electron. Syst.*, vol. 51, no. 2, pp. 1029–1038, Apr. 2015.

[14] B. Tang, J. Li, and J. Liang, "Alternating direction method of multipliers for radar waveform design in spectrally crowded environments," *Signal Process.*, vol. 142, pp. 398–402, 2018.

[15] A. Aubry, A. De Maio, M. Piezzo, M. M. Naghsh, M. Soltanalian, and P. Stoica, "Cognitive radar waveform design for spectral coexistence in signal-dependent interference," in *Proc. IEEE Radar Conf.*, 2014, pp. 0474–0478.
[16] A. Aubry, V. Carotenuto, and A. De Maio, "Forcing multiple spectral compatibility constraints in radar waveforms," *IEEE Signal Process. Lett.*, vol. 23, no. 4, pp. 483–487, Apr. 2016.
[17] G. Cui, X. Yu, Y. Yang, and L. Kong, "Cognitive phase-only sequence design with desired correlation and stopband properties," *IEEE Trans. Aerosp. Electron. Syst.*, vol. 53, no. 6, pp. 2924–2935, Dec. 2017.
[18] X. Yu, G. Cui, P. Ge, and L. Kong, "Constrained radar waveform design algorithm for spectral coexistence," *Electron. Lett.*, vol. 53, no. 8, pp. 558–560, 2017.
[19] W. Rowe, P. Stoica, and J. Li, "Spectrally constrained waveform design [sp tips &tricks]," *IEEE Signal Process. Mag.*, vol. 31, no. 3, pp. 157–162, May 2014.
[20] J. Liang, H. C. So, C. S. Leung, J. Li, and A. Farina, "Waveform design with unit modulus and spectral shape constraints via lagrange programming neural network," *IEEE J. Sel. Topics Signal Process.*, vol. 9, no. 8, pp. 1377–1386, Dec. 2015.
[21] H. He, P. Stoica, and J. Li, "Waveform design with stopband and correlation constraints for cognitive radar," in *Proc. 2nd Int. Workshop Cogn. Inf. Process.*, 2010, pp. 344–349.
[22] P. Ge, G. Cui, S. M. Karbasi, L. Kong, and J. Yang, "A template fitting approach for cognitive unimodular sequence design," *Signal Process.*, vol. 128, pp. 360–368, 2016.
[23] P. Stoica, H. He, and J. Li, "New algorithms for designing unimodular sequences with good correlation properties," *IEEE Trans. Signal Process.*, vol. 57, no. 4, pp. 1415–1425, Apr. 2009.
[24] P. Stoica, H. He, and J. Li, "On designing sequences with impulse-like periodic correlation," *IEEE Signal Process. Lett.*, vol. 16, no. 8, pp. 703–706, Aug. 2009.
[25] J. Song, P. Babu, and D. P. Palomar, "Optimization methods for designing sequences with low autocorrelation sidelobes," *IEEE Trans. Signal Process.*, vol. 63, no. 15, pp. 3998–4009, Aug. 2015.
[26] J. Liang, H. C. So, J. Li, and A. Farina, "Unimodular sequence design based on alternating direction method of multipliers," *IEEE Trans. Signal Process.*, vol. 64, no. 20, pp. 5367–5381, Oct. 2016.
[27] Y. Jing, J. Liang, D. Zhou, and H. C. So, "Spectrally constrained unimodular sequence design without spectral level mask," *IEEE Signal Process. Lett.*, vol. 25, no. 7, pp. 1004–1008, Jul. 2018.
[28] H. B. Yilmaz, T. Tugcu, F. Alagoz, and S. Bayhan, "Radio environment map as enabler for practical cognitive radio networks," *IEEE Commun. Mag.*, vol. 51, no. 12, pp. 162–169, Dec. 2013.
[29] W. Dinkelbach, "On nonlinear fractional programming," *Manage. Sci.*, vol. 13, no. 7, pp. 492–498, 1967.
[30] D. R. Hunter and K. Lange, "A tutorial on MM algorithms," *Amer. Statistician*, vol. 58, no. 1, pp. 30–37, 2004.
[31] Y. Sun, P. Babu, and D. P. Palomar, "Majorization-minimization algorithms in signal processing, communications, and machine learning," *IEEE Trans. Signal Process.*, vol. 65, no. 3, pp. 794–816, Feb. 2017.
[32] W. Fan, J. Liang, and J. Li, "Constant modulus MIMO radar waveform design with minimum peak sidelobe transmit beampattern," *IEEE Trans. Signal Process.*, vol. 66, no. 16, pp. 4207–4222, Aug. 2018.
[33] K. Shen and W. Yu, "Fractional programming for communication systems—Part I: Power control and beamforming," *IEEE Trans. Signal Process.*, vol. 66, no. 10, pp. 2616–2630, May 2018.
[34] J. Borde and J.-P. Crouzeix, "Convergence of a Dinkelbach-type algorithm in generalized fractional programming," *Zeitschrift für Operat. Res.*, vol. 31, no. 1, pp. A31–A54, 1987.
[35] S. Schaible, "Fractional programming. ii, on Dinkelbach's algorithm," *Manage. Sci.*, vol. 22, no. 8, pp. 868–873, 1976.
[36] M. Razaviyayn, M. Hong, and Z.-Q. Luo, "A unified convergence analysis of block successive minimization methods for nonsmooth optimization," *SIAM J. Optim.*, vol. 23, no. 2, pp. 1126–1153, 2013.
[37] J. A. Tropp, I. S. Dhillon, R. W. Heath, and T. Strohmer, "Designing structured tight frames via an alternating projection method," *IEEE Trans. Inf. Theory*, vol. 51, no. 1, pp. 188–209, Jan. 2005.
[38] D. P. Bertsekas, "Incremental gradient, subgradient, and proximal methods for convex optimization: A survey," *Optim. Mach. Learn.*, vol. 2010, no. 1–38, 2011, Art. no. 3.
[39] S. Boyd and L. Vandenberghe, *Convex Optimization*. Cambridge, U.K.: Cambridge Univ. Press, 2004.
[40] D. P. Palomar, J. M. Cioffi, and M. A. Lagunas, "Uniform power allocation in MIMO channels: A game-theoretic approach," *IEEE Trans. Inf. Theory*, vol. 49, no. 7, pp. 1707–1727, Jul. 2003.
[41] G. Scutari, D. P. Palomar, and S. Barbarossa, "Competitive design of multiuser MIMO systems based on game theory: A unified view," *IEEE J. Sel. Areas Commun.*, vol. 26, no. 7, pp. 1089–1103, Sep. 2008.
[42] G. Scutari, D. P. Palomar, and S. Barbarossa, "Cognitive MIMO radio," *IEEE Signal Process. Mag.*, vol. 25, no. 6, pp. 46–59, Nov. 2008.

Linlong Wu received the B.Eng. degree in electronic engineering from the Xi' an Jiaotong University, Xi'an, China, in June 2014, and the Ph.D. degree in electrical and computer engineering from the Hong Kong University of Science and Technology, Hong Kong, in November 2018. His research interests include optimization algorithms and signal processing with applications in radar, sensor networks, and financial engineering.

Daniel P. Palomar (S'99–M'03–SM'08–F'12) received the Electrical Engineering and Ph.D. degrees from the Technical University of Catalonia (UPC), Barcelona, Spain, in 1998 and 2003, respectively. During 2004–2006, he was a Fulbright Scholar with Princeton University, Princeton, NJ, USA. He is currently a Professor with the Department of Electronic & Computer Engineering and Department of Industrial Engineering & Decision Analytics, Hong Kong University of Science and Technology (HKUST), Hong Kong, which he joined in 2006. He previously held several research appointments, namely, at King's College London, London, U.K.; Stanford University, Stanford, CA, USA; Telecommunications Technological Center of Catalonia, Barcelona, Spain; Royal Institute of Technology, Stockholm, Sweden; University of Rome "La Sapienza," Rome, Italy; and Princeton University, Princeton, NJ, USA. His research interests include applications of optimization theory and signal processing in financial systems and big data analytics. He was a recipient of a 2004/06 Fulbright Research Fellowship, the 2004 and 2015 (co-author) Young Author Best Paper Awards by the IEEE Signal Processing Society, the 2015–16 HKUST Excellence Research Award, the 2002/03 best Ph.D. prize in Information Technologies and Communications by the UPC, the 2002/03 Rosina Ribalta first prize for the Best Doctoral Thesis in Information Technologies and Communications by the Epson Foundation, and the 2004 prize for the best Doctoral Thesis in Advanced Mobile Communications by the Vodafone Foundation and COIT. He has been a Guest Editor for the IEEE JOURNAL OF SELECTED TOPICS IN SIGNAL PROCESSING 2016 Special Issue on "Financial Signal Processing and Machine Learning for Electronic Trading", an Associate Editor for IEEE TRANSACTIONS ON INFORMATION THEORY and IEEE TRANSACTIONS ON SIGNAL PROCESSING, a Guest Editor for the IEEE SIGNAL PROCESSING MAGAZINE 2010 Special Issue on "Convex Optimization for Signal Processing," the IEEE JOURNAL ON SELECTED AREAS IN COMMUNICATIONS 2008 Special Issue on "Game Theory in Communication Systems, and the IEEE JOURNAL ON SELECTED AREAS IN COMMUNICATIONS 2007 Special Issue on "Optimization of MIMO Transceivers for Realistic Communication Networks."